

AD-A100 693

GENERAL ELECTRIC CORPORATE RESEARCH AND DEVELOPMENT --ETC F/8 14/2  
GAS DIAGNOSTIC MEASUREMENTS BY COHERENT ANTI-STOKES RAMAN SPECT--ETC(U)  
JUN 80 R L ST. PETERS, M LAPP F33615-77-C-3112

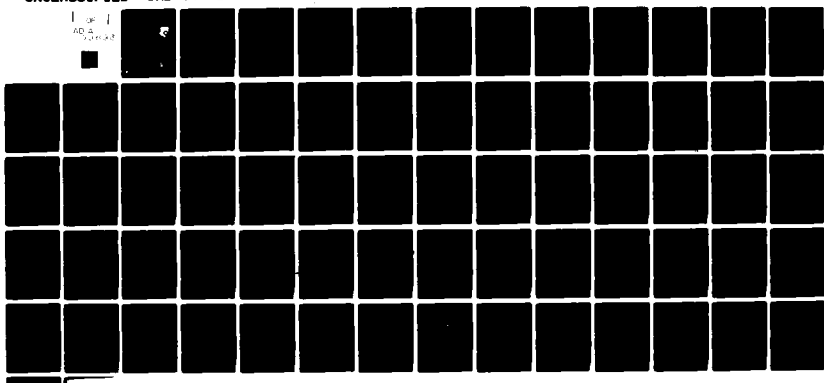
UNCLASSIFIED

SRD-81-023

AFWAL-TR-80-2062

NL

1 of 1  
ADA  
200002



END  
DATE  
FILED  
8-81  
DTIC

AFWAL-TR-80-2062

LEVEL 1  
S

**GAS DIAGNOSTIC MEASUREMENTS BY COHERENT ANTI-STOKES  
RAMAN SPECTROSCOPY: FEASIBILITY CALCULATIONS  
FOR WATER VAPOR IN COMBUSTION SYSTEMS**

AD A100693

GENERAL ELECTRIC COMPANY  
CORPORATE RESEARCH AND DEVELOPMENT  
COMBUSTION AND FUEL SCIENCE BRANCH - 115  
P.O. BOX 8  
SCHENECTADY, NEW YORK 12301



June 1980

TECHNICAL REPORT AFWAL-TR-80-2062  
FINAL REPORT FOR PERIOD 77 JUL 15 THROUGH 79 OCT 15

Approved for public release; distribution unlimited

AERO PROPULSION LABORATORY  
AIR FORCE WRIGHT AERONAUTICAL LABORATORIES  
AIR FORCE SYSTEMS COMMAND  
WRIGHT-PATTERSON AIR FORCE BASE, OHIO 45433

AMC FILE COPY

DTIC  
ELECTED  
S JUN 26 1981  
A

81 6 25 048

NOTICE

When Government drawings, specifications, or other data are used for any purpose other than in connection with a definitely related Government procurement operation, the United States Government thereby incurs no responsibility nor any obligation whatsoever; and the fact that the government may have formulated, furnished, or in any way supplied the said drawings, specifications, or other data, is not to be regarded by implication or otherwise as in any manner licensing the holder or any other person or corporation, or conveying any rights or permission to manufacture use, or sell any patented invention that may in any way be related thereto.

This report has been reviewed by the Office of Public Affairs (ASD/PA) and is releasable to the National Technical Information Service (NTIS). At NTIS, it will be available to the general public, including foreign nations.

This technical report has been reviewed and is approved for publication.



PAUL W. SCHREIBER  
Project Engineer



ROBERT R. BARTHELEMY  
Chief, Energy Conversion Branch  
Aerospace Power Division  
Aero Propulsion Laboratory

FOR THE COMMANDER



JAMES D. REAMS  
Chief, Aerospace Power Division  
Aero Propulsion Laboratory

"If your address has changed, if you wish to be removed from our mailing list, or if the addressee is no longer employed by your organization please notify \_\_\_\_\_, W-PAFB, OH 45433 to help us maintain a current mailing list".

Copies of this report should not be returned unless return is required by security considerations, contractual obligations, or notice on a specific document.

SECURITY CLASSIFICATION OF THIS PAGE (When Data Entered)

REPORT DOCUMENTATION PAGE		READ INSTRUCTIONS BEFORE COMPLETING FORM
1. REPORT NUMBER AFWAL-TR-80-2062	2. GOVT ACCESSION NO. AD-100693	3. RECIPIENT'S CATALOG NUMBER
4. TITLE (and Subtitle) GAS DIAGNOSTIC MEASUREMENTS BY COHERENT ANTI-STOKES RAMAN SPECTROSCOPY: FEASIBILITY CALCULATIONS FOR WATER VAPOR IN COMBUSTION SYSTEMS	5. TYPE OF REPORT & PERIOD COVERED Technical-Final; Period covered 77 Jul 15 through 79 Oct 15	
6. AUTHOR(S) R. L. St. Peters	7. PERFORMING ORG. REPORT NUMBER SRD-81-073	
8. CONTRACT OR GRANT NUMBER(S) F33615-77-C-3112	9. PERFORMING ORGANIZATION NAME AND ADDRESS General Electric Corporate Research & Development Center PO Box 8, Schenectady, NY 12301	
10. PROGRAM ELEMENT, PROJECT, TASK AREA & WORK UNIT NUMBERS 2301-S1-01	11. CONTROLLING OFFICE NAME AND ADDRESS Aero Propulsion Laboratory AF Wright Aeronautical Laboratories AFSC Wright-Patterson Air Force Base, OH 45433	
12. REPORT DATE June 1980	13. NUMBER OF PAGES 64	
14. MONITORING AGENCY NAME & ADDRESS (if different from Controlling Office) <i>(Signature)</i>	15. SECURITY CLASS. (of this report) Unclassified	
16. DISTRIBUTION STATEMENT (of this Report) Approved for public release; distribution unlimited.		
17. DISTRIBUTION STATEMENT (of the abstract entered in Block 20, if different from Report)		
18. SUPPLEMENTARY NOTES		
19. KEY WORDS (Continue on reverse side if necessary and identify by block number) Combustion diagnostics, cars spectra, water vapor spectrum, calculated spectra, nonlinear optics.		
20. ABSTRACT (Continue on reverse side if necessary and identify by block number) Coherent anti-Stokes spectroscopy (CARS) can be considerably simpler than is suggested by literature analyses based on interactions of monochromatic waves. The simplification arises when the optical properties of real lasers are incorporated into the analysis. To incorporate these properties, it is necessary to recognize that the underlying nonlinear optical interaction has a previously ignored complexity and is dependent on the coherence properties of the fields as well as on their spectra. The coherence of the interaction, as described by		

the CARS linewidth parameter, is degraded by the imperfect coherence of the laser sources. Whereas in conventional analyses the coherence of the interaction, which is the cause of the spectral complexity usually associated with CARS, is determined only by the sample and can be a strong function of sample conditions such as temperature, this coherence is in fact dependent on the apparatus as well, in the form of  $\Gamma_c = \Gamma_s + \Gamma_p + \Gamma_R$ .  $\Gamma_c$ ,  $\Gamma_s$ , and  $\Gamma_R$  are respectively the spontaneous Raman halfwidth and the mode halfwidths of the pump and Stokes lasers. The occurrence of the nonlinear interaction depends on the small size of laser mode widths, or more fundamentally, on the statistical degeneration of each incident field into a small number of independent fields, a property possessed only by optical fields from lasers.

If the lasers' contributions to the linewidth parameter are made dominant, the degree of coherence becomes a fixed property of the apparatus, simplifying interpretation of CARS spectra and extending the range of usefulness of CARS well beyond what would otherwise be expected. Available numerical values plus considerations of effects such as mode frequency chirp suggest that domination of the coherence by the apparatus can be arranged or at least approached in most cases. However, a few uncertainties remain, such as Doppler broadening, and numerically computed CARS spectra both of diatomic molecules and of water vapor show that some details must be considered.

## **FOREWORD**

This final technical report covers work performed under Contract F33615-77-C-3112 with the Department of the Air Force, Air Force Systems Command, Air Force Aero Propulsion Laboratory, Wright-Patterson Air Force Base, Ohio. The work was performed at Corporate Research and Development at the General Electric Company in Schenectady, New York. Work described herein covers the period from 15 July 1977 to 15 October 1979.

The program was under the direction of P. Schreiber of the Aero Propulsion Laboratory; this report was submitted in June, 1980.

Principal Investigator was M. Lapp. This report was prepared by R. L. St. Peters.

## Table of Contents

	<u>Page</u>
I. INTRODUCTION AND SUMMARY	1
I.A Introduction	1
I.B Overview	1
I.C Summary	5
II. THEORY	9
II.A Introduction	9
II.B Physical Model	10
II.C Deterministic Treatments	11
II.C.1 Coherent Treatments	11
II.C.2 Incoherent Treatments	13
II.C.3 A Gedanken Experiment	17
II.C.4 Multimode Lasers with Independent Modes	20
II.D Non-Determinism	26
II.D.1 Ergodicity	26
II.D.2 The Importance of Laser Modes	27
II.D.3 Stochastic Damping	29
II.E Non-Stationarity	30
II.F Doppler Broadening	32
III. CARS SPECTRA	36
III.A The CARS Susceptibility	36
III.B The Resonant Susceptibility for Vibrational Raman Bands	39
III.B.1 Diatomic Molecular Gases	39
III.B.2 Water Vapor	41
III.C Laser Mode Widths	43
III.D Raman Widths	44
III.E The CARS Linewidth Parameter	48
III.F Spectral Computations	50
III.G Conclusions	58
References	60

Application For	
REF ID: A7131	
Approved _____	
Justification _____	
By _____	
Distribution/ _____	
Availability Codes _____	
Avail and/or Dist      Special	
A	

THIS PAGE BLANK-NOT FILMED

## I. INTRODUCTION AND SUMMARY

### I.A. Introduction

CARS is an acronym for either coherent anti-Stokes Raman scattering or for coherent anti-Stokes Raman spectroscopy. The latter is an experimental technique based on the former, which is a physical process. The physical process was first reported in 1965 by Maker and Terhune<sup>1</sup>, and, to our knowledge, the earliest public description of CARS as a useful form of spectroscopy was in a paper presented by J.-P. E. Taran in May, 1973, at a Raman workshop on gas diagnostics<sup>2</sup>. CARS has since become a popular form of spectroscopy with multiple advantages, especially the strength and collimation of the scattered beam, and there have been a number of recent reviews<sup>3</sup>.

CARS can also have some significant disadvantages, primarily those related to the complexity of the dependence of CARS spectra on temperature, pressure, and species composition. This complexity arises because CARS spectra are the result of coherent interference among Raman resonances, and the linewidth parameter governing the spectral distance over which resonances interfere can itself be a complex function of the environmental parameters.

However, in this report we will see that CARS is an even more complex physical process than has been previously recognized, yet this increased complexity of CARS as a physical process can considerably simplify CARS as a form of spectroscopy.

### I.B. Overview

The course of work under this contract proceeded somewhat differently than envisioned at the outset. The original plan called for an initial study

of the factors influencing CARS spectra under flame conditions followed by the writing of two computer programs to calculate CARS spectra, first for diatomic molecules and then for water vapor.

However, it soon became evident that one of the primary tools needed to study CARS spectra is the ability to compute them. We therefore began developing the computer code early in the contract period. Recognizing that the core of the calculation is the same for all molecules, we decided upon a modular program architecture with which a single general program can compute spectra for any molecule by use of an appropriate variation of the subroutine module that supplies the data characterizing the molecule.

As we gained experience at computing spectra, it became more and more evident that the critical unknown is the linewidth parameter in the expression for the third-order susceptibility. Within the conventional theory, this parameter is simply the spontaneous Raman linewidth, so we examined the spontaneous Raman literature for relevant measurements and theory. We found measurements to be relatively sparse but the linewidth theory has been extensively developed and is in surprisingly good quantitative agreement with the best measurements. Although the theory is too complex for direct numerical computation of linewidths under flame conditions, it is a good guide as to how the Raman linewidths should scale with temperature, density, and some additional influences, primarily composition. The quantitative success of the theory for NTP (Normal Temperature and Pressure) gave us a certain measure of confidence in its prediction that the scaling should be roughly gas kinetic, with some additional decrease under flame conditions due to dilution.

At this stage of our effort, some CARS experimental results and associ-

ated spectral computations apparently inconsistent with this prediction were presented to us by Alan Eckbreth of UTRC (United Technologies Research Center) in an invited seminar here. Instead of the roughly  $T^{-1/2}$  temperature scaling we had expected for the Raman linewidth, the new results showed agreement between experimental flame spectra and spectra calculated using a constant linewidth parameter. While this was highly favorable for the practical use of CARS, there was no immediate explanation. However, at that time we had underway a small concurrent theoretical program with internal funding directed at a deeper understanding of CARS from a quite different approach. Shortly after the linewidth parameter discrepancy appeared, its resolution arose within this concurrent effort. However, although we had soon obtained a key mathematical result and interpreted it in simple physical terms, our understanding of this result is still evolving.

The element in our result that is most important to this contract is that the CARS linewidth parameter does not equal the spontaneous Raman linewidth. The CARS linewidth parameter is the sum of the spontaneous Raman linewidth plus additional terms that depend only on the apparatus, not on the sample conditions. When the apparatus' contribution is large, the CARS linewidth is effectively constant, although the Raman linewidth may vary considerably. (Recent measurements have in fact shown that spontaneous Raman linewidths are quite small in flames at one atm., as we had expected.) The CARS linewidth question is intricately related to another central issue: the role of the finite spectral widths of the source lasers. Because the modular architecture of our program allowed us to complete the programming phases more rapidly than anticipated, we were able to pursue these spectral issues toward the end of this contract. We discuss them at length in Section II.

In the programming phases, we began calculating CARS spectra early in the contract period. We initially made provision in the program for each line to have a different linewidth parameter, although we soon made a judgment that line-to-line variation was not likely to be important and that a common linewidth could be used for all lines in a band. As noted previously, we first expected this parameter to scale with gas-kinetic scaling, and we wrote such scaling into the program. Our later realization that this parameter depended on the lasers and would have to be supplied by the user resulted in a considerable simplification of the program.

As the program evolved, reflecting our developing understanding of CARS, we used it to calculate multiple CARS spectra, observing their degree of sensitivity to various parameters. The earlier spectra were all for diatomic molecules, principally N<sub>2</sub>. Roughly midway in the contract period we adapted the program to calculate spectra of water vapor by writing an appropriate subroutine module to provide the water vapor Raman data.

However, water vapor presented its own special problem. For diatomic molecules the program's DATA subroutine could calculate the input data from a handful of molecular constants. Calculation of this data for water vapor, however, is an intricate task, itself far more complex than calculation of a CARS spectrum. This task has been undertaken by a group at Orsay in France, and the only feasible procedure is to use their tabulated results. Initially we had on hand an early version of the French results and, after writing a DATA subroutine to read these results from a disc file, we were able to calculate low temperature water vapor CARS spectra.

This first dataset included no results for excited state bands. We next

obtained two additional datasets, both also originating from the Orsay group. One of these datasets has been published in the literature and contains extensive data on the first hot band as well as on the ground state band. We obtained the second of these two recent datasets from Professor R. Gaufres at Montpellier, also in France. This second recent dataset contains less extensive data for the first two bands but contains some data on higher excited state bands. The latter two sets thus complement each other. While there are small differences between these datasets where they overlap, our tests of the sensitivity of the CARS spectra to the precision of the data indicate these differences are too small to matter.

Water vapor CARS spectra have complex irregular structures, and, unlike diatomic spectra, water vapor spectra are sensitive to the shapes as well as the widths of the spectral broadening functions, particularly with regard to the relative height of the prominent central peak characteristic of these spectra.

### I.C. Summary

As a physical process, CARS is considerably more complex than has been generally recognized. CARS has a profound dependence on the statistical properties of the incident radiation, and although the statistical properties determine the source spectra, the spectra are not a sufficient description of these properties. For real sources, the generated CARS power is not simply a linear sum of the CARS powers for a distribution of monochromatic sources. The CARS power is, however, a linear sum of the CARS powers for the distribution of statistically independent non-monochromatic fields comprising the real source fields.

The sources for CARS are lasers, which have special statistical properties. If the lasers are stationary, each laser's output field is a sum of independent fields no more in number than the oscillating modes. These independent fields form a basis for an inner product space containing the laser's output field. The CARS power is a sum of a finite number of terms from interactions of various combinations of independent basis fields.

The most convenient basis may be used, and the mode fields form a basis if the modes are independent. While laser modes are never completely independent, they are usually only weakly coupled. Taking the mode fields to be an independent basis should usually be a good approximation, especially if the mode widths are relatively large. Modes with poor self coherence are unlikely to have much mutual coherence.

The CARS power is thus the sum of the powers arising from independent interactions of various mode combinations. The power resulting from any one combination of interacting modes is proportional to  $|\tilde{x}|^2$ , where  $\tilde{x}$ , defined in Eq. (II.23), has the same functional form as the susceptibility  $x$  for interacting monochromatic fields. The CARS susceptibility  $\tilde{x}$ , however, expresses the interaction in terms of mode center frequencies, not monochromatic frequency components, and its resonant terms have an augmented linewidth parameter  $\Gamma_c = \Gamma + \Gamma_p + \Gamma_s$  and a normalization factor  $(\Gamma_c/\Gamma)^{1/2}$ .

In a deterministic treatment of the CARS polarization, these simple modifications to the susceptibility are not exact for inter-resonance cross terms. However, the excitation of the medium in CARS is a resonant excitation by stochastic fields, is delayed, is integrated over time, involves energy storage, has memory of the field history (hysteresis), and is indeterminate in

terms of the current fields. In a treatment using a causal perturbation expansion and truly ergodic field averages, these simple susceptibility modifications are exact. The differences between this result and the deterministic result are irrelevant numerically but are important conceptually in that they help show the importance of laser sources.

CARS sources are roughly stationary over a response time of the medium but are not usually even approximately stationary over the full interaction time for pulsed lasers. The most probable type of change, chirp of the mode frequencies, is crudely equivalent to a larger effective mode width.

Doppler broadening can also affect CARS spectra, but it has not yet been adequately treated.

For diatomic molecules, the Raman data necessary to compute CARS spectra can be computed using the usual molecular constants. For water vapor, the Raman data must be stored in a tabulated form that can be read by the program that computes the spectrum.

The one important parameter that in general cannot be calculated or stored is the CARS halfwidth parameter, the sum of the spontaneous Raman halfwidth and the mode halfwidths, effective (chirp-related) or real, of the source lasers. The Raman width varies from line to line and depends on almost every environmental factor, but most of these dependencies are weak. For a given species, the Raman widths are about the same for all lines and roughly follow a gas kinetic scaling with temperature (and presumably with pressure). Even the Raman widths of different species (with the exception of H<sub>2</sub> gas, as is to be expected) do not seem to differ greatly.

The laser mode widths, on the other hand, may differ by several orders of magnitude. For measurement purposes, the most interesting case is when the mode widths (or effective chirp-induced widths) dominate the CARS linewidth parameter, because this parameter then becomes a property of the apparatus, essentially the same for all species. CARS spectra can then be computed with confidence for different species and a range of environments, to be compared with measured spectra.

Our spectral computations generally show good agreement with available experimental spectra. We have computed simulations that suggest that the rounded leading edges of some published experimental N<sub>2</sub> spectra are due to saturation effects. However, this leading edge saturation is due to the small statistical weights of the first few lines and would not affect spectral fits using other portions of the spectra. It may also be a useful saturation indicator. For water vapor, our computed spectra show that prominent spectral features can be sensitive to the shapes as well as the widths of spectral broadening functions.

## II. THEORY

### II.A. Introduction

There are numerous literature treatments of the CARS interaction of monochromatic sources, and we assume the reader is familiar with the description of CARS in such a context. In this section we are concerned with the influence of spectral properties of real sources, and we will see that we must also consider their coherence properties. At the beginning of the contract period, CARS using sources with finite spectral widths had been little discussed in the literature, except for a simplistic view of the broadband-Stokes CARS technique.

At about that same time we undertook an internally-funded effort to deepen our understanding of CARS. We did so with no intention or expectation of developing any significant advances in the theoretical treatment of CARS. Our goal was to answer for ourselves some questions we had about the way some things were done in the literature. However, this effort lead to a reformulation of the theory of CARS whose most prominent feature is an augmented linewidth parameter in the CARS susceptibility. This reformulation incorporated the points discussed in Section II.D., although it was some time before we understood all these points as they are presented in that section. As we tried to understand our own calculation and relate it to what had been done in the literature, we began to develop the "incoherent" treatment discussed in Section II.C.2. Although we did this independently, we were not the first. Prior to our work, Hall had developed an essentially similar treatment<sup>4</sup> and Hall and Eckbreth<sup>5</sup> had published the resulting spectral broadening equation. Others have also developed such treatments. However, to our

knowledge, the discussions in the rest of Section II.C. have not been developed by others. Section II.C.4. achieves the desired contact between this type of treatment and our original calculation.

## II.B. Physical Model

Although a simplistic theory of CARS can be developed in terms of the interaction of two monochromatic waves, CARS is fundamentally an interaction between three incident waves in a Raman-active medium, so let us consider the interaction of three fields  $E_1$ ,  $E_2$ , and  $E_s$  in a molecular gaseous medium. We assume  $E_1$  and  $E_2$  are components of the pump beam with roughly equal angular frequencies  $\omega_1$  and  $\omega_2$ ;  $E_s$  is a component of the Stokes beam with frequency  $\omega_s$  such that  $\omega_1 - \omega_s$  and  $\omega_2 - \omega_s$  are near or within a band of Stokes Raman shifts of the gas. The simplistic case with just two monochromatic waves corresponds to the degenerate case in which all three of these fields are monochromatic and  $\omega_1 = \omega_2$ . A Raman-active medium is necessarily nonlinear, and  $E_1$  beats with  $E_s$  to form a driving force at  $\omega_1 - \omega_s$  that drives the Raman-active molecular oscillations. The driven oscillations modulate the molecular polarizabilities, and these in turn modulate the polarization induced by the third field  $E_2$ , causing frequency sidebands. Because the driving forces are tied to the fields  $E_1$  and  $E_s$  and the induced polarizations are in response to  $E_2$ , the phases of the polarization sidebands of otherwise independent molecules are not independent. These mutually coherent anti-Stokes sideband polarizations sum to form a bulk polarization wave propagating in a direction determined by the incident field directions. This third-order polarization wave, at frequency  $\omega_a = \omega_1 - \omega_s + \omega_2$ , acts as a source radiating at  $\omega_a$ . The central theoretical problem in CARS is the formation of this third-order polarization, and we will spend most of this section discussing various semi-classical treatments,

although we will borrow concepts and insight from quantized treatments of the field.

This physical model for CARS resembles the common model for spontaneous Raman scattering. In the latter, it is spontaneous thermal oscillations that modulate the molecular polarizations, and the resulting polarization sidebands are mutually incoherent. We emphasize that the driven oscillations in CARS form only a minute increment to the concurrent thermal oscillations. The radiated power is so much larger for CARS only because these minute increments are mutually coherent and the fields radiated by an enormous number of molecules add in amplitude rather than intensity.

Many of the points we discuss in this section apply to nonlinear optics<sup>6,7</sup> in general, not simply to CARS.

### **II.C. Deterministic Treatments**

#### **II.C.1. Coherent Treatments**

The classic basic treatments of nonlinear optics were developed at a time when the laser was a novel new device whose output was clearly "monochromatic" by any prior standard. These treatments generally envisioned the fields involved as being a small number of essentially discrete and monochromatic laser emissions whose interactions were to be sorted out on a spectral scale characterized by sums and differences of their frequencies. In these treatments two or more monochromatic fields interact to form monochromatic nonlinear polarizations related to the fields by nonlinear susceptibilities.

There have been attempts<sup>8,9</sup> to treat spectral widths in nonlinear optics by identifying monochromatic Fourier components of spectrally broad fields

with the monochromatic source fields of these early treatments. The generated monochromatic polarization waves are then regarded as Fourier components of the nonlinear polarization, with the result for the CARS polarization

$$\tilde{P}_C(\omega) = \int d\omega_1 \int d\omega_s \int d\omega_2 \chi_C(\omega_1, \omega_s, \omega_2) \delta\{\omega - (\omega_1 - \omega_s + \omega_2)\} \\ \times \tilde{E}_1(\omega_1) \tilde{E}_s^*(\omega_s) \tilde{E}_2(\omega_2), \quad (II.1)$$

where  $\sim$  denotes a Fourier transform and  $\chi_C$  is the third-order susceptibility for CARS. The spectrum of the CARS polarization is taken to be proportional to  $|\tilde{P}_C(\omega)|^2$ .

According to this equation for  $\tilde{P}_C(\omega)$ , the field frequency components at a set of frequencies  $(\omega_1, \omega_s, \omega_2)$  interact to generate a frequency component at  $\omega = \omega_1 - \omega_s + \omega_2$ . The field freq at another set of frequencies  $(\omega_1 + \epsilon, \omega_s, \omega_2 - \epsilon)$  also generate a polarization component at the same  $\omega$ , and the characteristic feature of this type of treatment is that these two contributions, along with many others for other frequency combinations, are added in amplitude. In other words, they are all treated as being mutually coherent.

The field frequency components at the frequencies  $(\omega_1, \omega_s, \omega_2)$  actually generate two contributions to the polarization component at  $\omega = \omega_1 - \omega_s + \omega_2$ . One contribution comes from  $\omega_1$  and  $\omega_s$  beating together to drive a molecular oscillation at  $\omega_1 - \omega_s$  that in turn modulates the polarization induced by the  $\omega_2$  field component. The second contribution has the roles of the  $\omega_1$  and  $\omega_2$  field components interchanged and involves a molecular oscillation driven at  $\omega_2 - \omega_s$ . When these are added in amplitude, they imply a susceptibility with two terms. The susceptibility term from the first contribution is a function only of  $\omega_1 - \omega_s$  and that for the second term is the same function of  $\omega_2 - \omega_s$ . If we call this function  $x(\omega)$ , then

$$x_c(\omega_1, \omega_s, \omega_2) = x(\omega_1 - \omega_s) + x(\omega_2 - \omega_s) \quad (\text{II.2})$$

### **II.C.2. Incoherent Treatments**

A coherent treatment of linewidth fails to account for the stochastic element of radiation that gives rise to the property called incoherence. While this stochastic element is inherent in a quantized-field theory, it is not fully consistent with the basic classical description of radiation. However, classical coherence theory<sup>10,11,12,13</sup> has evolved methods for treating incoherent or partially coherent fields whose stochastic element is attributed to the statistical nature of a thermal source. These methods can be adapted to treat the inherent stochastic nature of radiation.

Each laser radiation field is treated as a narrowband random process - a harmonic wave with random fluctuations in its amplitude and phase. For the time scales of typical CARS experiments, transients may be neglected and the fields are treated as stationary. Observed physical quantities such as the spectrum of the CARS polarization are averages over time or, equivalently, over an ergodic ensemble. These averages are calculated as averages over amplitudes and phases of the laser fields. The result is that the contributions to each polarization frequency must be added incoherently, even the two contributions from each individual set of frequencies. The spectrum of the CARS polarization generated by the interaction of three beams is then

$$|\tilde{P}_c(\omega)|^2 = \left( \frac{8\pi}{c} \right)^3 \int d\omega_1 \int d\omega_s \int d\omega_2 \{ |x(\omega_1 - \omega_2)|^2 + |x(\omega_2 - \omega_s)|^2 \} \quad (\text{II.3})$$

$$\times \delta\{(\omega - (\omega_1 - \omega_s + \omega_2))\} I_1(\omega_1) I_s(\omega_s) I_2(\omega_2)$$

where  $I_1(\omega^1)$  is the intensity spectrum of  $E_1$ , etc. In the degenerate case of a single pump beam acting in both roles, the polarization spectrum has a single term,

$$|\tilde{P}_c(\omega)|^2 = \left(\frac{8\pi}{c}\right)^3 \int d\omega_1 \int d\omega_s \int d\omega_2 |x(\omega_1 - \omega_s)|^2 \\ \times \delta\{\omega - (\omega_1 - \omega_s + \omega_2)\} I_1(\omega_1) I_s(\omega_s) I_1(\omega_2). \quad (II.4)$$

As we will discuss shortly, the function  $x(\omega)$  is the same function, including overall numerical factors, in both Eq. (II.3) and (II.4). The intensity spectrum of the radiated CARS field is proportional to the polarization spectrum.

A point that must be emphasized is that although the polarization contributions of different sets of field frequency components are mutually incoherent, the contribution from any one set is itself still the coherent sum of contributions from different Raman lines. Although we have labelled this type of treatment as incoherent, the coherent interference between Raman resonances remains intact.

Although the first publication of an incoherent-summation spectral broadening equation was by Hall and Eckbreth<sup>5</sup>, they did not publish a derivation. The only incoherent treatment in the literature is a recent paper by Yuratich<sup>14</sup>. However, Yuratich considers only two limiting cases. In the early part of his paper, he derives an incoherent-summation spectral broadening equation, his Eq. (24), for the interaction of three independent fields with spectra such that any Raman-resonance between  $E_2$  and  $E_s$  is negligible. His susceptibility in his Eq. (6) thus has only one of the terms of our susceptibility in Eq. (II.2), and his Eq. (24) has only one term, corresponding to the first term of our Eq. (II.3). The other limit considered by Yuratich, in his Appendix B, is the degenerate limit of a single pump beam acting as both  $E_1$  and  $E_2$ .

However, whereas two pump fields well separated spectrally may be heuristically distinguished on a spectral basis, this distinction between them is

lost if they have overlapping spectra. A distinction between them, if one exists, can be made only on statistical grounds. The principle of superposition implies that their sum is fundamentally a single field, and we may treat the superposition  $E = E_1 + E_2$  as a single field with two statistically independent component fields. Applying the treatment for a single pump field in Yuratich's Appendix B, the correlation function in his Eq. (B8) becomes a sum of terms,

$$\begin{aligned} & \langle E(\omega_1)^* \tilde{E}(\omega_2)^* \tilde{E}(\omega'_1) \tilde{E}(\omega'_2) \rangle = \\ & \quad \langle \tilde{E}_1(\omega_1)^* \tilde{E}_1(\omega_2)^* \tilde{E}_1(\omega'_1) \tilde{E}_1(\omega'_2) \rangle \\ & \quad + \tilde{E}_2(\omega_1)^* \tilde{E}_2(\omega_2)^* \tilde{E}_2(\omega'_1) \tilde{E}_2(\omega'_2) \rangle \quad (\text{II.5}) \\ & \quad + \langle \tilde{E}_1(\omega_1)^* \tilde{E}_1(\omega'_1) \rangle \langle \tilde{E}_2(\omega_2)^* \tilde{E}_2(\omega'_2) \rangle \\ & \quad + \langle \tilde{E}_1(\omega_2)^* \tilde{E}_1(\omega'_2) \rangle \langle \tilde{E}_2(\omega_1)^* \tilde{E}_2(\omega_1) \rangle, \text{ etc.,} \end{aligned}$$

where, of the eight non-zero terms, only the four CARS terms have been displayed.

The first two terms on the right hand side express the interaction of each pump field with itself and give polarization spectra as in Eq. (II.4). The second two terms give the two polarization spectral terms of Eq. (II.3) for the interaction of two independent fields. The complete polarization spectrum arising from the four terms of Eq. (II.5) may be written

$$\begin{aligned} \tilde{P}_c(\omega)^2 &= P_{11,s}(\omega)^2 + P_{22,s}(\omega)^2 \\ &\quad P_{12,s}(\omega)^2 + P_{21,s}(\omega)^2 \quad (\text{II.6}) \end{aligned}$$

Thus, because the pump field is a sum of independent fields, the correlation function of Eq. (II.5) is a sum of terms, each term representing the indepen-

dent interaction of a set of independent fields. Each interacting set of fields makes an independent contribution to the overall spectrum. The spectral contribution of the cross-pump-field interaction is itself the sum of two independent contributions due to the two distinguishable pump roles.

Eq. (II.6) is a special case of a general principle. The pump field may consist of any number of independent component fields, in which case each pump field component independently interacts with itself and with each other pump field component. Furthermore, the Stokes field may also be a sum of independent components,  $E_s = \sum_k E_{s,k}$ . The Stokes autocorrelation function is then a sum of terms, one for each field component. There are two independent spectral contributions from each combination of two pump and one Stokes fields, plus one contribution from each degenerate interaction of one pump field with one Stokes field. The general spectral broadening equation is

$$|\tilde{P}_c(\omega)|^2 = \sum_i \sum_j \sum_k |P_{i,j,k}(\omega)|^2 \quad (\text{II.7})$$

where

$$|P_{i,j,k}(\omega)|^2 = \left(\frac{8\pi}{c}\right)^3 \int d\omega_1 \int d\omega_s \int d\omega_2 |x(\omega_1 - \omega_s)|^2 \\ \times \delta\{\omega - (\omega_1 - \omega_s + \omega_2)\} I_i(\omega_1) I_{s,k}(\omega_s) I_i(\omega_2) \quad (\text{II.8})$$

Note that the order of the indices is significant; each index position corresponds to one of the three beam roles in the interaction. For example, our earlier expression for three interacting beams, Eq. (II.3), is the sum of  $|P_{1,2,s}|^2$  plus  $|P_{2,1,s}|^2$ . We can see from Eq. (II.7) that the full interaction of the three beams must include terms with each pump beam interacting with itself as in Eq. (II.4)

### II.C.3. A Gedanken Experiment

We can gain some further insight into the physics underlying the mathematics of a treatment such as Yuratich's Appendix B by considering the gedanken experiment illustrated in Figure 1. In the experiment, the output of a cw pump laser with power  $P_d = 4P_0$  is split into two equal arms that are then recombined after a variable relative optical delay. This recombined pump beam interacts in a sample medium with a Stokes beam from a laser with power  $P_s$  and generates a CARS beam. For simplicity, we assume that each laser's output is a single statistically irreducible field, meaning that it cannot be separated into statistically independent parts. The results of the experiment, however, are in fact independent of this assumption. In one limiting case, the relative optical delay is large compared to a pump coherence time, and the recombined pump beam is actually two mutually incoherent spatially superimposed pump beams with equal power ( $P_0$ ) and identical spectra. The total pump power incident on the sample is  $2P_0$ , and another  $2P_0$  escapes at point A. The CARS beam is the incoherent sum of four independent contributions as in (Eq. II.6). The total CARS power is

$$P_{\text{inc}} = 2\alpha P_1 P_2 P_s + \beta P_1^2 P_s + \beta P_2^2 P_s = P_0^2 P_s (2\alpha + 2\beta) \quad (\text{II.9})$$

where  $\alpha$  and  $\beta$  incorporate the spectral integrations of Eqs. (II.3) and (II.4). Since the spectra are identical,  $\alpha = \beta$  but we distinguish between them for reference. In the second limiting case, the relative optical delay is zero. The arms recombine coherently to form a beam that is a single statistical unit and has all the power of the laser,  $P_d = 4P_0$ . The fields at point A cancel and no power escapes there. By Eq. (II.4), the total CARS power is then

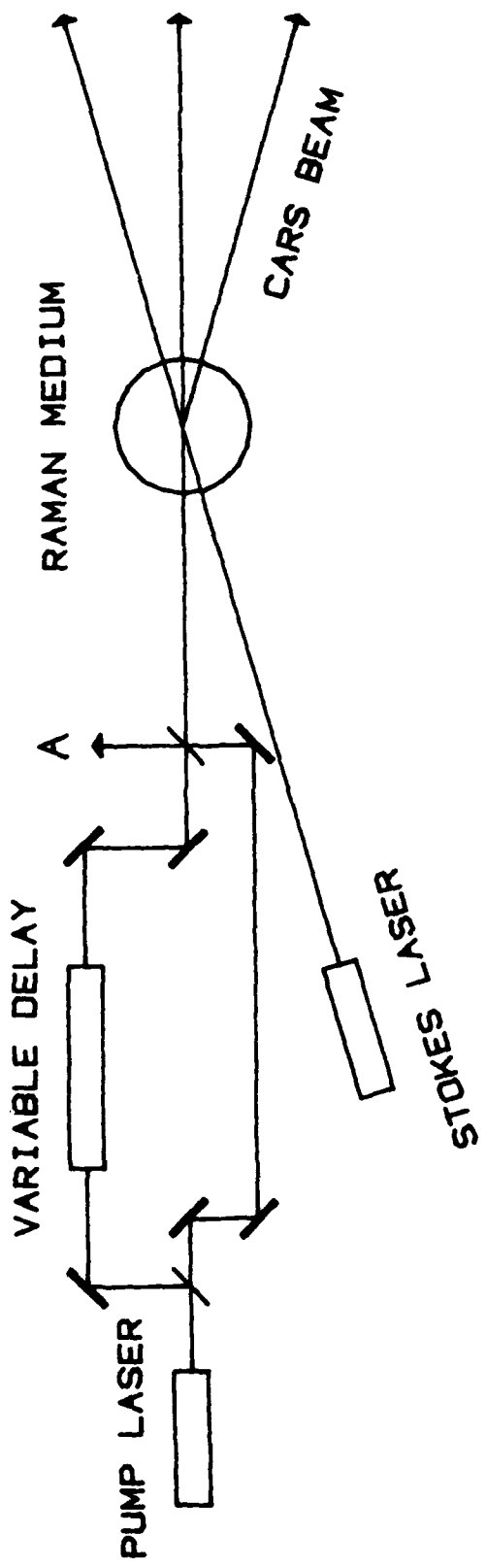


Figure 1 Schematic diagram of the gedanken experiment.

$$P_{coh} = \beta P_d^2 P_s = P_0^2 P_s (16\beta) \quad (II.10)$$

The power ratio for the two limits is

$$R = \frac{P_{coh}}{P_{inc}} = \frac{16\beta}{(2\alpha + 2\beta)} = \frac{8\beta}{\alpha + \beta}. \quad (II.11)$$

The requirement that  $\alpha$ ,  $\beta$  and  $R$  all be positive implies  $0 < R < 8$ . There is no simple definitive argument that can specify the ratio more precisely than these bounds, but intuition strongly suggests  $R = 4$ . This is also implied by the calculated relation  $\alpha = \beta$ , which in turn depends on the function  $\chi(\omega)$  being the same, including in particular overall numerical factors, in Eqs. (II.3) for non-degenerate mixing and Eq. (II.4) for the degenerate single pump beam case. By separating statistical degeneracy from simple spectral degeneracy, we have found that equal overall numerical factors in the susceptibility functions for the two cases is consistent with intuition.

In our large delay case, the total pump power incident on the sample is  $2P_0$  divided between two statistically independent pump beams with identical spectra, and the total CARS power generated is  $4\beta P_0^2 P_s$ . Since this equals  $\beta(2P_0)^2 P_s$ , it is the CARS power that would be generated by a single pump beam that could not be decomposed into two independent parts and that had the same spectrum and total power  $2P_0$ , such as our gedanken experiment in the zero delay case if we reduce the laser to half power. In other words, the total CARS power depends only on the total pump power and not on whether that pump power is in one beam or two beams. (This statement, however, is not necessarily true if a scalar treatment of the fields is not applicable, e.g., for two pump beams with different polarization states.)

Although the total CARS power is the same for a given pump power whether that pump power is in a single statistically irreducible beam or divided

between two independent beams, in the two beam case only half of the CARS power is due to interactions involving both pump beams. It is in this sense that a single pump beam interaction is "intrinsically stronger by a factor of two." However, if the two independent pump beams have identical spectra, the power generated by the interaction between them cannot be distinguished from the power generated by each beam interacting with itself<sup>15</sup>, and the total CARS power generated depends only on the total incident pump power.

#### II.C.4. Multimode Lasers with Independent Modes

The most important composite fields are the fields from multimode lasers. In Section II.D.2. we will briefly consider the possibility of correlations between these component modes, but in this section we will assume these modes are all statistically independent. Thus the broadband Stokes CARS arrangement, for example, involves a broad Stokes beam spanning a large number of Stokes modes. As a simple illustrative case, we assume the pump beam has a single mode with a Lorentzian profile centered at  $\omega_p$  and with halfwidth  $\Gamma_p$ , and we also assume the Stokes modes have Lorentzian profiles all with the same halfwidth  $\Gamma_s$ . We let  $\omega_k$  be the center frequency of Stokes mode  $k$ . According to (Eq. II.7) the CARS polarization spectrum for this example is

$$|\tilde{P}_c(\omega)|^2 = \sum_k |\tilde{P}_k(\omega)|^2 \quad (\text{II.12})$$

where  $|\tilde{P}_k(\omega)|^2$  is the spectral contribution from the interaction of Stokes mode  $k$  with the single pump mode. Thus the CARS output beam has one mode for each incident Stokes mode. However, both the incident Stokes and output anti-Stokes spectra are usually measured with inadequate resolution to observe these modes. The measured spectral profiles are locally averaged profiles. With a spectrometer set at frequency  $\omega_0$ , the observed CARS power is

$$P_c(\omega_0) = C \int d\omega F(\omega - \omega_0) |\tilde{P}(\omega)|^2 = C \sum_k \int d\omega F(\omega - \omega_0) |\tilde{P}_k(\omega)|^2 \quad (\text{II.13})$$

where  $F(\omega)$  is the spectrometer slit function and  $C$  is the proportionality constant between the CARS power and the absolute value squared of the CARS polarization.

Assuming the slit function is wide compared to the spectral width of an anti-Stokes mode, we can write this as:

$$P_c(\omega_0) = C \sum_k F(\omega_k - \omega_0) \int d\omega |\tilde{P}_k(\omega)|^2 = C \sum_k F(\omega_k - \omega_0) P_k \quad (\text{II.14})$$

where  $P_k$  and  $\omega_k$  are the integrated CARS polarization power and mode center frequency for anti-Stokes mode  $k$ . From Eq. (II.8),

$$P_k = \left(\frac{8\pi}{c}\right)^3 \int d\omega_s \int d\omega_2 |\chi(\omega_k - \omega_2)|^2 I_{s,k}(\omega_s) I_p(\omega_2) \int d\omega_1 I_p(\omega_1) \quad (\text{II.15})$$

The  $\omega_1$  integral is simply the integrated intensity  $I_p$  of the pump beam, whereas the  $\omega_s$  and  $\omega_2$  integrals are a double convolution. If the susceptibility is due to a single resonance at  $\Omega$ , then it has a Lorentzian profile and can be written

$$|\chi(\omega)|^2 = \frac{x_0^2 \pi}{\Gamma} L_\Gamma(\omega - \Omega) \quad (\text{II.16})$$

where  $L_\Gamma$  is a normalized Lorentzian with halfwidth  $\Gamma$ , and  $x_0$  is a constant. The convolutions in Eq. (II.15) are then convolutions of Lorentzians, and using the general relation

$$\int d\omega_1 L_{\Gamma_1}(\omega_1 - \omega) L_{\Gamma_2}(\omega) = L_{\Gamma_1 + \Gamma_2}(\omega) \quad (\text{II.17})$$

Eq. (II.15) becomes

$$P_k = \left(\frac{8\pi}{c}\right)^3 I_p^2 I_{s,k} \frac{x_0^2 \pi}{\Gamma} L_{\Gamma_c}(\Omega - \omega_k) \quad (\text{II.18})$$

where<sup>6</sup>

$$\Gamma_c = \Gamma + \Gamma_p + \Gamma_s \quad (\text{II.19})$$

In the usual broadband-Stokes CARS arrangement, the Stokes spectral envelope is roughly constant, so we take  $I_{s,k}$  to be independent of mode number  $k$ ,  $I_{s,k} = I_s$ . Then by approximating the sum over  $k$  with an integral, Eq. (II.14) becomes

$$P_c(\omega_0) = \left(\frac{8\pi}{c}\right)^3 c \frac{I_s^2}{\Delta\omega_s} \int d\omega F(\omega - \omega_0) |\tilde{x}(\omega)|^2 \quad (\text{II.20})$$

where  $\Delta\omega_s$  is the Stokes mode spacing and

$$|\tilde{x}(\omega)|^2 = |\tilde{x}_0|^2 L_{\Gamma_c}(\omega), \quad (\text{II.21})$$

$$\tilde{x}_0 = (\Gamma_c/\Gamma)^{1/2} x_0. \quad (\text{II.22})$$

The quantity  $I_s/\Delta\omega_s$  is the constant spectrally averaged Stokes intensity that would be measured with resolution inadequate to see the Stokes mode structure.

A similar analysis for a multimode pump laser shows that the final result is the same as Eq. (II.20) with  $F(\omega)$  replaced by

$$\frac{1}{\Delta\omega_p} \int d\omega_1 F(\omega - \omega_1) S_p(\omega_1)$$

where  $\Delta\omega_p$  is the pump mode spacing and  $S_p(\omega)$  is the normalized pump laser spectral envelope.

If there is more than a single resonance, then  $|x(\omega)|^2$  is not a single simple Lorentzian. There are then cross terms between resonances. These cross terms have the form

$$\frac{x_i}{(\Omega_i - \omega) - i\Gamma} \times \frac{x_j}{(\Omega_j - \omega) + i\Gamma}$$

For these terms one must not only substitute  $\Gamma_c$  for  $\Gamma$  but must also include an extra factor that approximately equals one. Hall<sup>4</sup> has shown that, for  $x_i = x_j$

this factor is

$$1 + i \frac{\Gamma_p + \Gamma_s}{\Omega_i - \Omega_j + i\Gamma}$$

This correction is not only negligible for any real CARS spectrum, it is applicable only to a theoretical development following the principles described in Section II.B.2. In Section II.C we will describe some shortcomings of this type of treatment. In a treatment incorporating the points we will raise, this correction factor does not appear. Eq. (II.20) thus gives the measured CARS spectrum for multiple Raman resonances, with

$$\tilde{x}(\omega) = (\Gamma_c/\Gamma)^{1/2} \sum_j \frac{x_j}{\Omega_j - \omega - i\Gamma_c} \quad (\text{II.23})$$

The dominant feature of Eq. (II.20) is the increase in the CARS linewidth parameter in  $\tilde{x}(\omega)$ . In a simplistic view, the Stokes laser spectrum would be regarded as constant over the Raman resonances, and a simple application of Eq. (II.4) leads to an expectation of a CARS spectrum proportional to  $|x(\omega)|^2$  with a CARS linewidth parameter equal to the spontaneous Raman linewidth. However, recognition that the observed "constant" Stokes spectrum is actually the envelope of the spectra of a large number of independent modes of equal intensity implies that the overall interaction is the sum of multiple independent interactions of individual modes. The observed anti-Stokes spectrum is the variation of the strengths of these interactions with the center frequencies of the Stokes modes involved. The linewidth parameter in the susceptibility describing this variation is the sum of the spontaneous width of a resonance plus a contribution from the apparatus equal to the sum of the widths of the interacting pump and Stokes laser modes. The CARS spectral envelope observed by the spectrometer is proportional to  $|\tilde{x}(\omega)|^2$ , the square of the same susceptibility function but with this larger linewidth parameter.

This linewidth parameter governs the spectral range over which the Raman resonances interfere, and it governs spectral features on a spectral scale much coarser than its actual value. Thus, although the spectrometer resolution may be poor compared to the mode widths or Raman width, the overall spectral envelope measured with the spectrometer can be sensitive to the value of the CARS linewidth parameter.

Another way to view the meaning of the augmented linewidth expression is to compare the broadband Stokes technique with the tuned CARS technique. In a tuned CARS experiment with single-mode lasers the resolution limit is determined by the laser spectral widths, i.e., the widths of their single modes. A single Raman resonance with halfwidth  $\Gamma$  would be observed as a peak that is the double convolution of the resonance with the two mode profiles. In other words it would be a Lorentzian with halfwidth  $\Gamma_c = \Gamma + \Gamma_p + \Gamma_s$ . Thus  $\Gamma_c$  is an inherent resolution limit for a CARS measurement of the resonance frequency, with three terms, two representing stochastic fluctuations in the fields and one representing collision-induced stochastic fluctuations in the induced oscillation. A broadband-Stokes CARS measurement is the simultaneous rather than sequential use of a large number of Stokes modes. The augmented linewidth expression says that the fundamental resolution limit is the same for both the scanned and broadband techniques.

#### **II.D. Non-Determinism**

##### **II.D.1. Ergodicity**

The fundamental average for the correlation functions in a classical treatment of the fields is a time average. The physical basis for the use of an ensemble average is that as the field amplitudes and phases fluctuate, the

fluctuating system "samples" a series of systems in an ensemble. The time average is then the same as the average over the sampled systems, and as the interaction time and therefore the number of systems sampled increases, this average becomes the same as the average over the whole ensemble. This physical basis is stated with mathematical rigor by the Ergodic Theorem. However, the theorem applies only if the ensemble meets certain requirements. Whereas ergodicity is a complex topic, we can loosely state simply that ergodicity requires that all expected behaviors of the physical system be represented in the ensemble. The average used by Hall and by Yuratich<sup>14</sup> in their incoherent treatments does not meet this test. Although this has negligible numerical relevance to CARS experiments to date, it has considerable conceptual implications affecting analysis of some extensions of these experiments, such as use of incoherent broadband Stokes sources.

According to the physical model for CARS, two fields  $E_1$  and  $E_s$  beat together to drive an oscillation at  $\omega_1 - \omega_s$ , which then modulates the polarization induced by  $E_3$ . A key element of this process is that the molecular oscillation represents the time-integrated effect of the driving force due to  $E_1$  and  $E_s$ , and energy is stored in this oscillation. If we consider the time interval immediately following a fluctuation in the driving fields, the amplitude and phase of the oscillation cannot immediately respond. The electrons respond almost instantaneously, but the nuclear Raman oscillation response is essentially determined by how rapidly collisional disruptions destroy the "memory" of the previous fields. The medium thus has a finite response time that is the inverse of the Raman linewidth. During this response time, the CARS polarization differs from the polarization appropriate for the new field amplitudes and phases. This combination of fields and CARS polarization is

therefore not represented by any system in an ensemble of systems with non-fluctuating fields. Averaging over an ensemble of systems with fixed amplitudes and phases is thus equivalent to leaving out of the time average all the time intervals immediately following fluctuations. Averaging over phases and amplitudes of the fields is not an ergodic average.

The basic interaction being averaged involves propagating monochromatic waves, not just field frequency components. The full ergodic ensemble must have all possible amplitudes and phases of the propagating waves, and this ensemble includes off-axis spatial components because fluctuations in a propagating wave introduce spatial as well as frequency broadening. We may in principle obtain an ergodic average by calculating the interaction for fields with fixed amplitudes and phases of a distribution of spatial components and averaging this interaction over the full ergodic ensemble. However, we may retain the convenience of considering only time variation by calculating the interactions of waves represented as individual spatial components with time varying amplitudes and phases and then averaging over all time histories, rather than simply over all values, of the amplitudes and phases. Only the second approach is feasible in practice. For reference, we will call this the fluctuating ensemble approach and will refer to an ensemble with constant phases and amplitudes as a coherent ensemble, because the individual systems in a coherent ensemble have fields with no stochastic content. An important element of a fluctuating ensemble approach is that the polarization is non-deterministic in the sense that it depends on the field history as well as on the current field.

### **II.D.2. The Importance of Laser Modes**

How much a coherent ensemble average differs from a time average obviously depends on the field fluctuation rate. If the broadband Stokes laser field were truly a single statistically irreducible field, the fluctuation rate corresponding to its spectral width would be extremely large, so large that not only would the amplitude and phase average differ greatly from a time average, but the field would also be unable to maintain coherence long enough to build up any driven molecular oscillation. There would be virtually no CARS signal at all.

Because the Stokes laser field is not statistically irreducible and is generally a superposition of statistically independent mode fields, the CARS interaction is a sum of multiple interactions, each of which is averaged separately. Each of these individual mode interactions has a fluctuation rate determined by the spectral width of an individual mode, not by the overall spectral width. When the mode widths are very small compared to the spontaneous Raman linewidths, these individual coherent interactions between modes have time to develop to the maximum extent allowed by collisions without disruption by a field fluctuation. A significant overall CARS interaction can develop only as the sum of multiple individual interactions of spectrally narrow modes. Thus the normally unresolved mode structure underlying the measured constant Stokes spectral envelope is necessary for the very existence of a significant CARS interaction. We can express the same statement in quantum terms by saying that a laser is a device that divides its output among a small enough number of discrete modes to give them sufficiently large occupation numbers to cause nonlinear optical effects.

Because the fluctuation rate of each individual mode interaction is small, the coherent-ensemble average used by Hall and Yuratich is a sufficiently accurate basis for numerical spectral calculations relevant to typical CARS experiments, provided the multimode structure is acknowledged by use of the augmented linewidth parameter of Eq. (II.19). What this augmented linewidth expresses physically is that the time available for  $E_1$  and  $E_s$  to build up the molecular oscillation is the time until either a disruptive collision or a field fluctuation, whichever comes first. The randomizing effect of either event is the same, and the stochastic elements from collisional disruption and imperfect field coherence are additive.

We first obtained the linewidth expression in Eq. (II.19) early in the contract period but as part of a separate internally-funded program to review the theoretical foundations of CARS. In that calculation we made use of the inherent mode structure of the laser fields to replace the continuous Fourier expansion integrals with analogous field expansions as discrete sums of laser mode fields. Each mode field was monochromatic except for amplitude and phase fluctuations, and the orthogonality of Fourier components was replaced by the statistical independence of the laser modes. Calculation of the individual mode interactions gave the linewidth expression of Eq. (II.19).

If the laser modes are not statistically independent, the calculation is more complex but not fundamentally different. First we note that the correlation function between two fields satisfies all the requirements for an inner product, and therefore the set of all linear combinations of the laser modes forms an inner product space spanned by the laser modes, whether or not the modes are independent. Next we note that a mode that is a monochromatic wave except for amplitude and phase fluctuations is a statistically irreducible

field: it cannot be decomposed into a sum of statistically independent fields. The number of dimensions of the inner product space is therefore no larger than the number of modes, say  $N$ , and since the field of interest is in the space, it consists of no more than  $N$  independent fields. Thus the field of a laser can always be written as the sum of a finite number of statistically independent and irreducible fields, and the CARS interaction is always a sum of interactions of independent field combinations, although the independent fields may each have contributions from more than one mode. However, if the laser modes have widths large enough for the correction to the CARS linewidth parameters to be important, they have relatively poor self-coherence, and we can expect such modes to have little intermode correlation.

#### II.D.3. Stochastic Damping

There is an additional form of non-determinism that has little relevance to the spectral calculations of this contract. We mention it here because it turns up in the results of a revised analysis of CARS theory incorporating the points we have been discussing in Section II.C. and because it helps further illustrate the considerable complexity of the CARS interaction.

Even for fields without fluctuations the polarization response is not unique. For example, if the fields are monochromatic,  $E_1$  and  $E_s$  form a monochromatic driving force for the molecular oscillations, and this force acts in competition with collisional damping. For truly smooth and continuous damping, the molecular oscillation would be monochromatic at the driving force frequency. However, for stochastic collisional damping, each molecule's oscillation is undamped between collisions. Following a disruptive, collision a molecule will spontaneously oscillate; initially at its natural frequency,

and the driving force takes a finite time to re-exert its influence. In spectral terms, we can summarize the result by stating that the CARS polarization response has a finite spectral width even if the incident fields are truly monochromatic. More importantly however, the polarization is not uniquely determined even if the past history of the fields is rigidly related to the present fields. The CARS medium itself is stochastic and non-deterministic.

### II.E. Non-Stationarity

In this section we have assumed that the fields can be treated as stationary. Since gases at NTP have response times of about 0.1 ns and typical CARS experiments use pulselengths around 10 ns, it should be a good approximation to treat the fields as stationary over a response time. We can thus consider the basic CARS interaction as an interaction of stationary modes, as we have done. However, we can expect the mode widths and center frequencies to vary during the course of the pulse, and the usual time-integrated CARS measurement is, in effect, a measurement of an average over these variations.

A mode with random fluctuations in its center frequency is analogous to a radio carrier with white noise frequency modulation. Such modulation results in a Lorentzian frequency probability distribution, and random frequency fluctuations are thus equivalent to a larger mode width. A more important form of variation in a mode center frequency is a systematic chirp. We can then divide the pulse into a number  $N$  of time intervals, where  $N$  is the pulselength divided by the medium's response time. For our typical case of a 10 ns pulse and a 0.1 ns response time we thus have  $N = 100$ . During the  $j$ th interval, our three incident interacting modes have frequencies  $\omega_{1,j}$ ,  $\omega_{2,j}$ , and  $\omega_{s,j}$  and intensities  $I_{1,j}$ ,  $I_{2,j}$  and  $I_{s,j}$ .

Assuming the variations in the center frequency of the CARS mode are not resolved, the average power in this mode due to the three incident fields acting in their familiar order is

$$\bar{P} = \frac{K}{N} \sum_{j=1}^N I_{1j} I_{sj} I_{2j} |\tilde{\chi}(\omega_{1j} - \omega_{sj})|^2 \quad (\text{II.24})$$

where K is an overall constant.

We have arrived at this equation by considering a physical situation in which the frequency triplets  $(\omega_{1,j}, \omega_{2,j}, \omega_{s,j})$  appear in order. However, the same equation would result if the frequency triplets appeared in any order, provided the frequencies with index j always appear with the intensities with index j. Alternatively,  $\bar{P}$  could be the average over a much larger number of frequency variations where the intensities remain constant but the product  $I_{1j} I_{sj} I_{2j}$  of our intensities is proportional to the number of times the jth frequency triplet appears.

In other words Eq. (II.24) is equivalent to taking the interaction between modes with a frequency difference  $\omega_j = \omega_{1j} - \omega_{sj}$  and averaging that interaction over a distribution of  $\omega_j$ 's. The effective spectral distribution is determined by the time variation of actual pulse intensities and by the chirp rates (which may vary). An integral approximation to Eq. (II.24) is a convolution of this chirp-induced effective spectral profile with  $|\tilde{\chi}(\omega)|^2$ . If the effective profile were Lorentzian, the result would be simply another addition to the effective susceptibility linewidth parameter. However, the chirp-induced profile will not generally be Lorentzian. Nevertheless, since the spectral profile of the generated CARS modes is not generally of interest, we can expect that a reasonable first approximation to the effect of chirp of the mode center frequencies is an increase in the effective mode width and in

the linewidth parameter in  $\tilde{\chi}$ . Thus Eq. (II.19) becomes approximately

$$\Gamma_{c,\text{eff}} = \Gamma + \Gamma_{p,\text{eff}} + \Gamma_{s,\text{eff}} \quad (\text{II.25})$$

where  $\Gamma_{p,\text{eff}}$  and  $\Gamma_{s,\text{eff}}$  are effective mode widths increased by chirp of the mode center frequencies.

For steady mode center frequencies, the effects of variations in the mode widths are more complex. However, for the narrowband lasers used as pump lasers for CARS, we would not expect much variation of the mode widths during a pulse. On the other hand, the broadband dye lasers used as Stokes laser might well have modes that start out rather broad but narrow significantly after a few cavity round trip times, i.e., toward the end of the pulse. However, the effects of any such behavior are likely to be offset by mode frequency chirp and its attendant increase in the effective mode width.

#### II.F. Doppler Broadening

Until recently, it was generally accepted that the CARS Doppler width is smaller than the spontaneous Raman Doppler width by a factor of  $\sqrt{2}$ . Then, in May, 1979, a paper by Bjarnason, Hudson, and Andersen<sup>17</sup> (BHA) presented a quantum theory of CARS lineshapes predicting a Doppler width about 1.2 times the spontaneous Raman Doppler width. However, we believe the BHA calculation is open to question.

BHA describe the radiation in terms of occupation numbers for plane wave states. They consider only interactions in which both pump photons come from the same plane wave state, whereas the plane wave decomposition of a real pump beam includes a distribution of plane wave states due both to its finite spectral width and to its finite spatial extent. The real CARS interaction cannot

be expressed as a superposition of interactions with each pump plane wave component interacting only with itself. Instead, the overall CARS interaction involves all pairs of pump plane wave components interacting with each other.

However, a more important criticism of the BHA calculation concerns its treatment of the gas. BHA take as their basis states direct products of one-molecule states, each of which is itself a product of an internal state and a free-molecule plane wave translational state. In a critical step, they then take these basis states to also be eigenstates of the unperturbed hamiltonian of the gas, in effect taking that hamiltonian to be a sum of free-molecule hamiltonians and neglecting collisions. It is this step that we most question.

The immediate effect of this step is that BHA can take the unperturbed density matrix to be diagonal in their basis states. This in turn causes the sum over final states in their Eq. (2.27) for the scattering rate to reduce to a single term in which the initial and final state of every molecule are identical. This identity between initial and final states of every molecule becomes the condition for intermolecular scattering coherence. Since it requires conservation of the momentum of the radiation, it also gives the phase matching condition.

However, BHA begin by totally neglecting collisions, and their result for the origin of the phase matching condition is simplistic. To see this, consider the dominant interaction term corresponding to a diagram with four photon interaction vertices at times  $t_1$ ,  $t_2$ ,  $t_3$ , and  $t_4$ . At  $t_1$ , the molecule absorbs a pump photon; at  $t_2$ , it is stimulated to emit a Stokes photon; at  $t_3$ , it absorbs another pump photon; and at  $t_4$ , it emits an anti-Stokes photon.

This diagram is to be integrated over all  $t_1 < t_2 < t_3 < t_4 < t$ . Assuming the gas has no absorption transition near the pump frequency, the first vertex does not conserve energy, and the uncertainty principle requires that the stimulated emission out of the first virtual intermediate internal state occurs almost instantly, so the time interval between the  $t_1$  and  $t_2$  vertices is essentially infinitesimal. Similarly, the time interval between the  $t_3$  and  $t_4$  vertices is equally minute. It is probably a reasonable approximation to neglect any interaction diagrams involving collisions during these intervals.

Since CARS is a resonant process, the intermediate internal state between the  $t_2$  and  $t_3$  vertices is a real state. Neglecting any radiative decay, the only limit to how long a molecule can stay in this state on resonance is the time to the next inelastic collision. In other words, even though the overall interaction is still treated as a net transition from one initial quantum state to another, the intermediate resonance allows the overall transition to span a finite time. During this time, the molecule can undergo elastic collisions, exchanging momentum with the surrounding gas. This change in momentum will prevent the final translational state from being the same as the initial state. According to the BHA result for the origin of intermolecular scattering coherence, these events with elastic collisions would not be part of the coherent scattering that is CARS.

That implication is not consistent with experiment, because Dicke narrowing<sup>18</sup> has been observed for CARS<sup>19</sup>. Dicke narrowing requires that collisions can occur with sufficient rapidity to reduce the effective molecular motion to diffusion and yet not affect the basic radiative process. Since any inelastic collision causes lifetime broadening of the radiation, such collisions must necessarily be elastic. The degree of motional damping required to produce

the observed Dicke narrowing implies that these elastic collisions involve large momentum changes. Observation of Dicke narrowing for CARS thus implies that events with different initial and final translational states can contribute to coherent scattering.

Elastic collisions are more frequent than inelastic collisions, and because it is the inelastic collision time that determines how long the interaction can span, there is always time for elastic collisions no matter how dilute the gas. It is never a good approximation to treat the molecular translational states as non-interacting. Through elastic collisions each molecule is coupled to the surrounding gas, which forms a momentum reservoir.

By summing the interaction amplitude over all molecules with randomly distributed positions and random collisional momentum changes, Silverstein<sup>20</sup> has obtained the usual phase matching condition, which now expresses separate momentum conservation for the radiation and for the gas as a whole but not for individual molecules. We have not yet extended Silverstein's calculation to the point where we can make any definitive statements about the extent of Doppler broadening, and we believe that experience has shown that an analysis of Doppler broadening must be done with considerable care and may involve subtle issues yet to be noticed. With that caveat, we can say that Silverstein's calculation appears to suggest that Doppler broadening will be smaller for CARS than for spontaneous Raman scattering.

### III CARS SPECTRA

#### III.A. THE CARS SUSCEPTIBILITY

The basic spectral quantity is the third-order CARS susceptibility. We have seen in Eq. (II.23) that the effective susceptibility  $\tilde{\chi}(\omega)$  depends on the apparatus through the linewidth parameter. However, for the moment we consider only the "intrinsic" susceptibility  $\chi(\omega)$ . For a molecular gaseous medium, we can generally divide  $\chi(\omega)$  into a resonant part and a nonresonant part. The resonant part is<sup>9</sup>

$$\chi^R(\omega) = \sum_k \frac{x_k}{\Omega_k - \omega - i\Gamma_k} \quad (\text{III.1})$$

where the sum is over the Raman resonances in the spectral region of interest. The  $x_k$  depend only very slowly on  $\omega$ . The halfwidths  $\Gamma_k$  may differ somewhat but generally not significantly. We will discuss them in Section III.D.

The nonresonant part of  $\chi(\omega)$  is itself a sum of two different kinds of contributions, Raman and two-photon contributions. The Raman contribution is the sum over all other Raman resonances of terms like those in Eq. (III.1). These resonances are all outside the spectral range of interest and therefore are individually small. There may be a considerable number of such terms, not only from other Raman bands of the electronic ground state, but also from transitions within the vibrational-rotational structure of excited electronic states. There may also be terms from electronic Raman scattering, and, although such terms may be intrinsically strong, they are particularly far from resonance, which considerably discounts their intrinsic strength.

The sum in EQ. (III.1) is over individual Raman transitions and the index  $k$  represents a set of quantum numbers of both the initial and final states.

As we will soon discuss, the vibrational Q-branch transitions of interest to us are dominated by "symmetric" or "trace" scattering in which the vibrational quantum numbers of the two states differ, but all the other quantum numbers, including the orientation quantum numbers, of the two states are the same. For a given vibrational quantum number change, the matrix element and transition frequency are independent of the orientation quantum number, depending only on the overall angular momentum quantum number  $j$ . We can then sum all the transitions with the same  $j$ . The result is identical with Eq. (III.1) except the label on each term is now  $j$ , and the strength factor  $x_j$  must include a statistical weight factor equal to the number of orientation terms for that  $j$ . This statistical weight factor is most fundamentally associated with the collection of transitions labelled by  $j$  although, since we are considering Q-branch transitions, it also equals the equal statistical weights of the initial and final rotational state manifolds.

A general expression for the strength factors is<sup>9</sup>

$$x_j = \frac{N\Delta_j W_j \alpha_j^2}{h} \quad (\text{III.2})$$

where  $\alpha_j$  and  $W_j$  are respectively the polarizability matrix element and statistical weight for transition  $j$ , and  $N\Delta_j W_j$  is the difference between the number densities of the molecules in the lower and upper states.  $N$  is the total molecular number density.

The non-resonant Raman terms all have the same basic form as the resonant susceptibility terms, assuming this dispersion function form is still applicable very far from resonance, and this has an interesting implication. Since all the Raman terms are due to transitions between vibrational-rotational states of one electronic state, or in the case of electronic Raman scattering,

of two different electronic states, they should all have roughly the same linewidth  $\Gamma$ . If we then consider the effective susceptibility  $\tilde{\chi}$ , every one of these terms has its  $\chi_j$  strength factor replaced by  $(\Gamma_c/\Gamma)^{1/2}\chi_j$  and its linewidth parameter replaced by  $\Gamma_c$ . Since these terms are far from resonance, the linewidth parameter replacement is irrelevant and the net effect is that the Raman portion of the non-resonant susceptibility is multiplied by  $(\Gamma_c/\Gamma)^{1/2}$ . The background CARS due to the square of this part of the non-resonant susceptibility is thus larger by a factor of  $(\Gamma_c/\Gamma)$ . On the other hand, the square of a resonant term is  $\chi_j^2/\Gamma^2$  before the replacements but becomes  $(\Gamma_c/\Gamma)(\chi_j^2/\Gamma_c^2) = (\Gamma/\Gamma_c)(\chi_j^2/\Gamma_2)$  with the replacements. Thus the resonant term is reduced by  $(\Gamma/\Gamma_c)$  while the background is raised by the same factor. The resonant-signal to nonresonant-background ratio is reduced by  $(\Gamma/\Gamma_c)^2$ . This is one undesirable effect of the augmented linewidth parameter that may partially offset some of its advantages, particularly in cases where the major part of the background is due to another species present in much higher concentration and with Raman resonances that are not very remote spectrally. The two-photon absorption transition contributions to the nonresonant susceptibility have a different spectral structure, being independent of  $\omega$ . There should be no need for rescaling of the nonresonant susceptibility due to these terms. Furthermore, even the rescaling of the background susceptibility due to remote Raman resonances is highly dependent on the extensive tails of Lorentzian profiles. An increase in the linewidth parameter that represents a first-order approximation to the effect of a chirp-induced increase in the effective mode width would not cause any rescaling of the background susceptibility.

### III.B. The Resonant Susceptibility for Vibrational Raman Bands

#### III.B.1 Diatomic Molecular Gases

For the Q-branch, only the vibrational state changes. The square of the matrix element depends on the vibrational transition. For an ideal harmonic oscillator<sup>21</sup>,

$$|\alpha_v|^2 = (v+1)|\alpha_0|^2 \quad (\text{III.3})$$

where  $\alpha_v$  is the matrix element for the  $v \rightarrow v+1$  transition. For a real diatomic molecule, Eq. (III.3) is a good approximation.

The ground state band matrix element  $\alpha_0$  is related to the spontaneous Raman scattering cross section  $d\sigma/d\Omega$  for this band<sup>9</sup>,

$$|\alpha_0|^2 = \frac{c^4}{\omega_s^4} \frac{d\sigma}{d\Omega} \quad (\text{III.4})$$

To be more precise, for our scalar treatment of the susceptibility the cross section in Eq. (III.4) is for linearly polarized incident light, non-depolarized Raman scattering, and scattering direction perpendicular to the incident polarization. Published experimental cross sections are generally for the total scattered power in both polarizations. However, because the depolarized Q-branch scattering from simple molecules is usually only a few percent of the total Q-branch scattering<sup>22</sup>, the total Q-branch cross section can be used directly in Eq. (III.4) with little error, generally to within the uncertainty in the total cross section. For example, the depolarized component for N<sub>2</sub> gas near NTP is less than two percent<sup>23</sup>.

A variation of the cross section sometimes encountered, usually in theoretical work, is the cross section relating photon scattering rate to

incident photon flux density, rather than scattered power to incident intensity. If this cross section variation is used, the factor of  $\omega_s^4$  in Eq. (III.4) should be  $\omega_p \omega_s^3$ .

The statistical weight of any line  $Q(J)$  of the Q-branch of a diatomic molecule is<sup>24</sup>

$$W_J = (2J+1)g_J \quad (\text{III.5})$$

where  $g_J$  is a nuclear spin state factor. This equation is correct only for the Q-branch component that comes from the trace of Placzek's<sup>25</sup> scattering tensor and is called either trace scattering or symmetric scattering. However, because the other Q-branch component, due to the "asymmetric" or "quadrupole" part of the scattering tensor, is only a very small fraction of the total, Eq. (III.5) is an excellent overall approximation for  $W_J$ . The nuclear spin weight factor  $g_J$  depends on the nuclear spins and results in an alteration of intensities.

If  $E_v$  is the vibrational energy of the lower vibrational state of the  $v \rightarrow v+1$  vibrational Raman band, and  $E_{v,J}$  is the rotational energy of the  $J$ th rotational substate, the number density of molecules in the lower state for the  $Q_v(J)$  line is

$$N_{v,J}(T) = N \frac{\exp(-E_v/KT)}{Z_{v,J}(T)} \frac{\exp(-E_{v,J}/KT)}{Z_{v,J}(T)} W_J \quad (\text{III.6})$$

where  $Z_v(T)$  and  $Z_{v,J}(T)$  are the appropriate partition functions. The rotational state energies are very nearly the same for state  $v$  and state  $v+1$ , and it is a good approximation to let

$$Z_{v,j}(T) \sim Z_J(T) \quad (\text{III.7})$$

where  $Z_J(T)$  is a single rotational partition function usable for all the

incident photon flux density, rather than scattered power to incident intensity. If this cross section variation is used, the factor of  $\omega_s^4$  in Eq. (III.4) should be  $\omega_p \omega_s^3$ .

The statistical weight of any line  $Q(J)$  of the Q-branch of a diatomic molecule is<sup>24</sup>

$$W_J = (2J+1)g_J \quad (\text{III.5})$$

where  $g_J$  is a nuclear spin state factor. This equation is correct only for the Q-branch component that comes from the trace of Placzek's<sup>25</sup> scattering tensor and is called either trace scattering or symmetric scattering. However, because the other Q-branch component, due to the "asymmetric" or "quadrupole" part of the scattering sensor, is only a very small fraction of the total, Eq. (III.5) is an excellent overall approximation for  $W_J$ . The nuclear spin weight factor  $g_J$  depends on the nuclear spins and results in an alteration of intensities.

If  $E_v$  is the vibrational energy of the lower vibrational state of the  $v \rightarrow v+1$  vibrational Raman band, and  $E_{v,J}$  is the rotational energy of the Jth rotational substate, the number density of molecules in the lower state for the  $Q_v(J)$  line is

$$N_{v,J}(T) = N \frac{\exp(-E_v/KT)}{Z_{v,J}(T)} \frac{\exp(-E_{v,J}/KT)}{Z_{v,J}(T)} W_J \quad (\text{III.6})$$

where  $Z_v(T)$  and  $Z_{v,J}(T)$  are the appropriate partition functions. The rotational state energies are very nearly the same for state  $v$  and state  $v+1$ , and it is a good approximation to let

$$Z_{v,j}(T) \sim Z_j(T) \quad (\text{III.7})$$

where  $Z_j(T)$  is a single rotational partition function usable for all the

vibrational states involved. Then

$$N\omega_j \Delta_{v,J}(T) = N_{v,J}(T) w_j \{1 - \exp(-\hbar\omega_{v,J}/KT)\}, \quad (\text{III.8})$$

where  $\omega_{v,J}$  is the frequency of the  $Q_v(J)$  line. Since we can calculate  $E_v$ ,  $E_{v,J}$  and  $\omega_{v,J}$  from standard molecular constants, we can also calculate  $N\Delta_{v,J}(T)$ .

We can thus calculate the susceptibility strength factors

$$\chi_{v,J}(T) = \frac{c^4}{\hbar\omega_s^4} \frac{d\sigma}{d\Omega} (2J+1) g_J N\Delta_{v,J}(T) \quad (\text{III.9})$$

that go into the resonant susceptibility of Eq. (III.1),

$$\chi_T^R(\omega) = \sum_{v,J} \frac{\chi_{v,J}(T)}{\Omega_{v,J} - \omega - i\Gamma_{v,J}(T)} \quad (\text{III.10})$$

Although  $N\Delta_{v,J}(T)$  and therefore  $\chi_{v,J}(T)$  depend on the energy levels as calculated from molecular constants, the principle sensitivity of the susceptibility to the accuracy of these constants is through the calculated Raman frequencies  $\Omega_{v,J}$  in the denominator.

### III.B.2 Water Vapor

Water is an asymmetric-top molecule with an energy level structure considerably more complicated than that of a simple diatomic molecule. Due to the asymmetry, there is considerable vibration-rotation interaction, and the vibrational structure alone involves three vibrational modes. The  $v_1$  and  $v_3$  modes have similar frequencies, and the  $v_2$  mode frequency is about half the other two. As a result of these relationships and the elaborate rotational structure of the vibrational states, there are complex Fermi resonances among various sets of vibrational levels. The calculation of the various vibrational-rotational state energies is a complex task that has been

undertaken with ever increasing sophistication during recent years by Flaud and Camy-Peret. The only feasible approach to calculating the susceptibility is to make use of their tabulated computed and measured energy levels.

The strong Raman-active vibrational band for water vapor is the  $v_1$  band. The simple series of diatomic molecule hot bands is replaced by a set of excited state bands, with the  $(v_1, v_2, v_3)$  band being the  $(v_1, v_2, v_3) \rightarrow (v_1+1, v_2, v_3)$  transition. At flame temperatures, where these excited state bands become important, it is necessary to consider the possibility that the matrix elements may depend on  $v_2$  or  $v_3$ . However, earlier work<sup>26</sup> on spontaneous Raman scattering from water vapor indicated that any such dependence is insignificant, and the agreement between our calculated CARS spectral profiles and experimental CARS spectra from the literature tends to confirm this.

At the beginning of this contract we had on hand early results of Flaud and Camy-Peret for the ground state band. We have since acquired two sets of more recent results of Flaud and Camy-Peret, one of which has been published<sup>27,28,29</sup>. We obtained the second of these datasets by courtesy of Prof. R. Gaufres at Montpellier, France. These two more recent datasets are complementary in that the unpublished dataset contains results for higher excited state bands, whereas the published dataset has results for higher J values for the lower bands. For lines common to these datasets, they generally agree to within  $0.01 \text{ cm}^{-1}$ . These datasets have been combined into a single dataset with all the necessary parameters for a total of 977 Raman lines in the  $(0,0,0)$ ,  $(0,1,0)$ ,  $(0,0,1)$ ,  $(0,1,1)$ , and  $(1,0,0)$  bands.

The statistical weights of water Raman lines are similar to those of dia-

tomic molecule lines as given in Eq. (III.5). However, for water vapor the nuclear spin state factor depends not on  $J$  but on the projection quantum number<sup>24</sup>  $\tau$ ,

$$W_{J\tau} = (2J+1)g_\tau \quad (\text{III.11})$$

where  $g_\tau = 1$  for odd  $\tau$  and  $g_\tau = 3$  for even  $\tau$ . With this change in the nuclear state factor, the calculation of the susceptibility for water vapor is basically the same as for diatomic molecules. The differences are that the state and transition energies are from pre-calculated input datasets, that the labeling of the transitions requires the additional indices  $\tau$ ,  $v_2$ , and  $v_3$ , and that the  $(v+1)$  factor in the square of the matrix elements becomes  $(v_1+1)$ .

### III.C Laser Mode Widths

Few measurements of mode widths for pulsed lasers are available. However, the single-mode Q-switched ruby laser used by Roh and Schreiber<sup>9</sup> as a pump laser for CARS has a mode halfwidth  $\Gamma_p = 17 \times 10^{-3} \text{ cm}^{-1}$  (510 MHz), which can be characterized as relatively large. On the other hand, the mode width for Q-switched Nd:YAG lasers of the type used by Eckbreth<sup>5</sup> is apparently determined essentially by the pulse duration, resulting in very narrow modes with halfwidths of the order of  $1 \times 10^{-3} \text{ cm}^{-1}$  (30 MHz). It is not clear whether these modes chirp, and they may therefore have an effective width for CARS that is larger. However, it is likely that the pump laser mode widths, real or effective, are smaller than the widths of the Stokes laser modes.

The Stokes laser is typically a broadband dye laser pumped by a portion of the pump beam. Because such a laser has a very large unsaturated gain and short characteristic time constants, the output pulse is essentially synchronous with the pump pulse even though the cavity transit time is a significant

fraction of the pulse length. (For a 50 cm cavity the one-way transit time is more than fifteen percent of a ten nanosecond pulselength.) Thus the Stokes pulse is emitted during the dynamic development of the spectral structure of the modes. The onset of lasing is analogous to a phase transformation, and only the "condensed phase" of the emission (i.e., the collimated beam rather than the fluorescence) is used for CARS. This collimated beam necessarily has a mode structure, but that structure evolves as the pulse develops. The mode structure development is subject to inherent and external perturbations such as (nonuniform) heating of the dye solution and mirror vibration.

We believe that the mode halfwidths of these Stokes lasers will generally be larger than the  $17 \times 10^{-3} \text{ cm}^{-1}$  halfwidth of the single-mode pump laser used by Roh and Schreiber. Since the mode separation for a 50 cm cavity is only  $10 \times 10^{-3} \text{ cm}^{-1}$ , the Stokes laser modes will generally have considerable spectral overlap. In this regard we emphasize that the distinction between the mode fields in the discussion in Chapter II is on the basis of statistical independence. Although some of that discussion is most easily visualized in terms of spectrally separated modes, spectral separation is unnecessary.

### III.D Raman Widths

If we ignore Doppler broadening for the moment, the halfwidth of a spontaneous Raman transition, when expressed in angular frequency units, equals the rate at which collisions disrupt the transition. There is no specific theory of collisional broadening directly applicable to water vapor. However, the theory of collisional broadening of Raman transitions of diatomic molecules has been extensively developed by Van Kronendonk and his co-workers<sup>30</sup> and by others<sup>31</sup> and is in surprisingly good quantitative agree-

ment with available experimental measurements.

This theory examines the perturbations of molecules due to various types of interactions between them as they pass near each other. While the theory itself is far too complex to discuss here, we can outline some general features.

Intermolecular collisions can affect Raman transitions only if they alter the internal state of the molecule. Most such collisions are inelastic, but because the internal energy is independent of the angular momentum quantum number  $M$ , a collision can change  $M$  and still be elastic. However, such collisions do not broaden the  $\Delta M = 0$  symmetric (or "trace") scattering transitions that comprise all but a few percent of the Q-branch. Since the state energies are independent of  $M$ , the transition energies are also independent of  $M$ , and a change in  $M$  causes no change in the transition energy. An alternative view is that since  $M$  enters the wave function in the exponent of a phase factor, a change in  $M$  results in the same phase change in the initial and final states and thus no net dephasing of the transition. Since all Raman transitions except vibrational Q-branch transitions are due to asymmetric (quadrupole) scattering, for which  $\Delta M \neq 0$  and which is broadened by these elastic collisions, the Q-branch broadening is less than that of the O and S branches and of pure rotational Raman scattering. Most linewidth measurements have been for rotational Raman scattering due to its large separation between relatively strong individual lines, but it is the Q-branch linewidths that are of most interest for CARS. Fortunately, the theory indicates that the elastic phase interrupt collisions cause only about fifteen percent of the broadening of asymmetric scattering<sup>32</sup>, so the collision linewidths of both symmetric and asymmetric scattering are approximately equal, and both are due primarily to

inelastic collisions.

The collision rates tend to be largest for inelastic collisions in which the internal energies of the colliding molecules change little. Most inelastic collisions therefore change only the rotational states. Because the rotational state energy differences are smaller for low-J states, these states tend to have higher inelastic collision cross sections.

However, a collision in which the molecules have substantial rotational energy changes can have a relatively large probability if the molecules simply exchange rotational energy with little transfer of energy between translation and rotation. This kind of collisional resonance can only occur in collisions between molecules with approximately equal rotational energy, and the probability a molecule will encounter another molecule with equal rotational energy is greatest for molecules in the most probable rotational state. This collisional resonance effect therefore tends to offset the decrease in the collision cross section with J. Detailed theoretical calculations generally yield Raman linewidths that decrease slowly with J at room temperature. However, because the most probable rotational state depends on temperature, the collisional resonance effect also implies that the J dependence of the collision broadening is different at different temperatures.

Due to collisional resonance, self-broadening of a gas is greater than broadening of the gas from collisions with molecules of other gases. The linewidths of a gas in a mixture are thus smaller than for the pure gas at the same pressure. With a reduction of the extent to which collisional resonances offset the decrease in broadening with increasing J, we can expect linewidths in mixtures to have a greater dependence on J, and we can also then expect the

decrease with  $J$  to remain as the temperature rises and the molecular population shifts to higher  $J$  states. The average linewidth of a gas in a mixture should therefore decrease with temperature somewhat more rapidly than a gas kinetic collision rate scaling, the scaling expected if the average collision cross section were constant. Furthermore since a collision cross section depends on the nature of the collision partner, the Raman linewidths of gases in a mixture depend on the composition of the mixture as well as the total pressure and temperature.

Raman linewidth measurements are not easy, and there have been relatively few, with  $N_2$  gas being the most common sample. Jammu, et al<sup>33</sup> measured pressure self-broadening coefficients for  $N_2$  rotational Raman lines at room temperature. Extrapolated to one atm. pressure, their data imply Raman halfwidths decreasing smoothly from a little over  $50 \times 10^{-3} \text{ cm}^{-1}$  for  $J = 2$  to a little over  $30 \times 10^{-3} \text{ cm}^{-1}$  for  $J = 16$ . Fletcher<sup>34</sup> has measured linewidths directly for the  $N_2$  Q-branch and also for the S-branch. Fletcher's measured values are somewhat larger, varying between  $50 \times 10^{-3}$  and  $75 \times 10^{-3} \text{ cm}^{-1}$  for most Q-branch lines and averaging about  $85 \times 10^{-3} \text{ cm}^{-1}$  for the S branch. However, Fletcher's linewidths have an irregular  $J$  dependence that seems unlikely, and little information other than his final results is yet available about his measurements.

Jammu et al also measured the self-broadening of  $O_2$  and  $CO_2$  and the foreign gas broadening of  $N_2$  and  $O_2$  by Ar and by He. They found the  $O_2$  self-broadening to be essentially the same as that of  $N_2$  whereas the  $CO_2$  self-broadening is approximately twice as great. The foreign gas experiments confirm that foreign gas broadening is less than self-broadening but only by about thirty to forty percent in the most extreme case they measured ( $N_2 +$

Ar). These foreign gas measurements thus suggest that the dependence of the linewidths on composition is not large.

The preceding measurements were all at room temperature. Owyong and Rahn<sup>36</sup> have made some N<sub>2</sub> Raman linewidth measurements at flame temperatures of the order of 1800 K, observing halfwidths around  $15 \times 10^{-3} \text{ cm}^{-1}$ . Little other information about these measurements is available. However, if we scale even the relatively small halfwidths of Jammu et al according to the T<sup>-1/2</sup> gas kinetic constant-pressure scaling from 1500 K to 300 K, we find somewhat larger predicted flame temperature halfwidths for all lines except those with the largest J values.

While the information about some of these measurements and the probable accuracy of all of them is inadequate to attach great significance to the exact values described here, they are adequate to establish the approximate size of room temperature Raman linewidths and to confirm that these linewidths scale roughly as the gas kinetic collision rate.

### III.E. The CARS Linewidth Parameter

In the preceding two sections we have seen that Raman linewidths and laser mode widths can be numbers of comparable size. Thus all three terms in the CARS linewidth parameter of Eq. (II.19),  $\Gamma_c = \Gamma + \Gamma_p + \Gamma_s$ , may be important. If the laser mode frequencies chirp during the pulse, the approximate effect is an even greater relative importance of the laser terms as discussed in Section II.E. Eq. (II.19) then gives way to Eq. (II.25),  $\Gamma_{c,\text{eff}} = \Gamma + \Gamma_{p,\text{eff}} + \Gamma_{s,\text{eff}}$ . These extra terms in the CARS linewidth parameter can considerably simplify the interpretation of CARS spectra, because they reduce the relative importance of variations in the spontaneous

Raman linewidth.

In the simplest limit, the spontaneous Raman halfwidth  $\Gamma$  is small compared to the sum of the laser mode halfwidths for all expected sample conditions. Then  $\Gamma_c = \Gamma + \Gamma_p + \Gamma_s \sim \Gamma_p + \Gamma_s$  and the augmented CARS linewidth parameter is the same for all lines of all species under all expected conditions. In other words, it has become a property of the apparatus, not of the scattering medium. If the mode widths are reduced, the next level of approximation is reached when the spontaneous Raman halfwidths are no longer negligible but the differences between the widths of different species are still negligible. Then  $\Gamma_c \sim \Gamma_0 + \Gamma_p + \Gamma_s$  where  $\Gamma_0$  is an average spontaneous halfwidth approximating the spontaneous halfwidth of any species.

For somewhat smaller mode widths, the next level of approximation is when the differences between species may be significant but the variations in Raman width of a single species over its various lines and over the expected range of environmental parameters can still be neglected. Then  $\Gamma_{c,x} \sim \Gamma_{0,x} + \Gamma_p + \Gamma_s$  for species  $x$ , where  $\Gamma_{0,x}$  is a constant average linewidth for species  $x$ .

In the latter two cases, it may be desirable to use a  $\Gamma_0$  or  $\Gamma_{0,x}$  that is not constant as the environmental parameters vary but instead scales according to gas kinetic scaling with temperature and total pressure. Whether constant values or values with gas kinetic scaling are used, these levels of approximation all maintain the highly desirable feature that the linewidth parameters are independent of composition. There is therefore no coupling of the spectra of different species through the linewidth parameter.

Relatively large mode widths clearly have certain advantages. For example, one can measure temperature by comparing computed and measured CARS spectra without knowing the temperature dependence or J dependence of the spontaneous Raman widths. Shirley, Eckbreth, and Hall<sup>36</sup> have had just such success with flame temperature measurements using CARS spectra computed with a constant linewidth (halfwidth) parameter  $\Gamma_c = 50 \times 10^{-3} \text{ cm}^{-1}$  for N<sub>2</sub> in flames, whereas the measurements of Owyong found a spontaneous Raman halfwidth around  $15 \times 10^{-3} \text{ cm}^{-1}$ . Although there is no direct evidence, we believe this success to be due to a comparatively large Stokes laser mode width, whether intrinsic or apparent as a result of chirp, for their laser-pumped dye-laser Stokes laser.

### III.F. Spectral Computations

Figure 2 shows an example of a computed CARS spectrum for N<sub>2</sub> gas at 1700°K. The spectrum has been folded with a gaussian spectrometer slit function with a FWHM of one  $\text{cm}^{-1}$ . The CARS halfwidth parameter is  $50 \times 10^{-3} \text{ cm}^{-1}$  and the standard molecular constants from Herzberg<sup>37</sup> were used. For this illustrative example, zero background susceptibility was used.

Due largely to the work of Eckbreth, Hall, and coworkers at UTRC<sup>38</sup> both experimental and computed spectra similar to Figure 2 are now familiar in the literature and have been much discussed. Over most of their spectral range, the computed and experimental spectra agree well. The one feature we will discuss is the small peak that rises above the bulk of the ground state band at its high frequency edge. This small peak is characteristic of our computed diatomic molecule spectra and of similar spectra computed by the UTRC group. However, this peak is absent from the UTRC experimental spectra, which generally have a rounded maximum and high frequency edge.

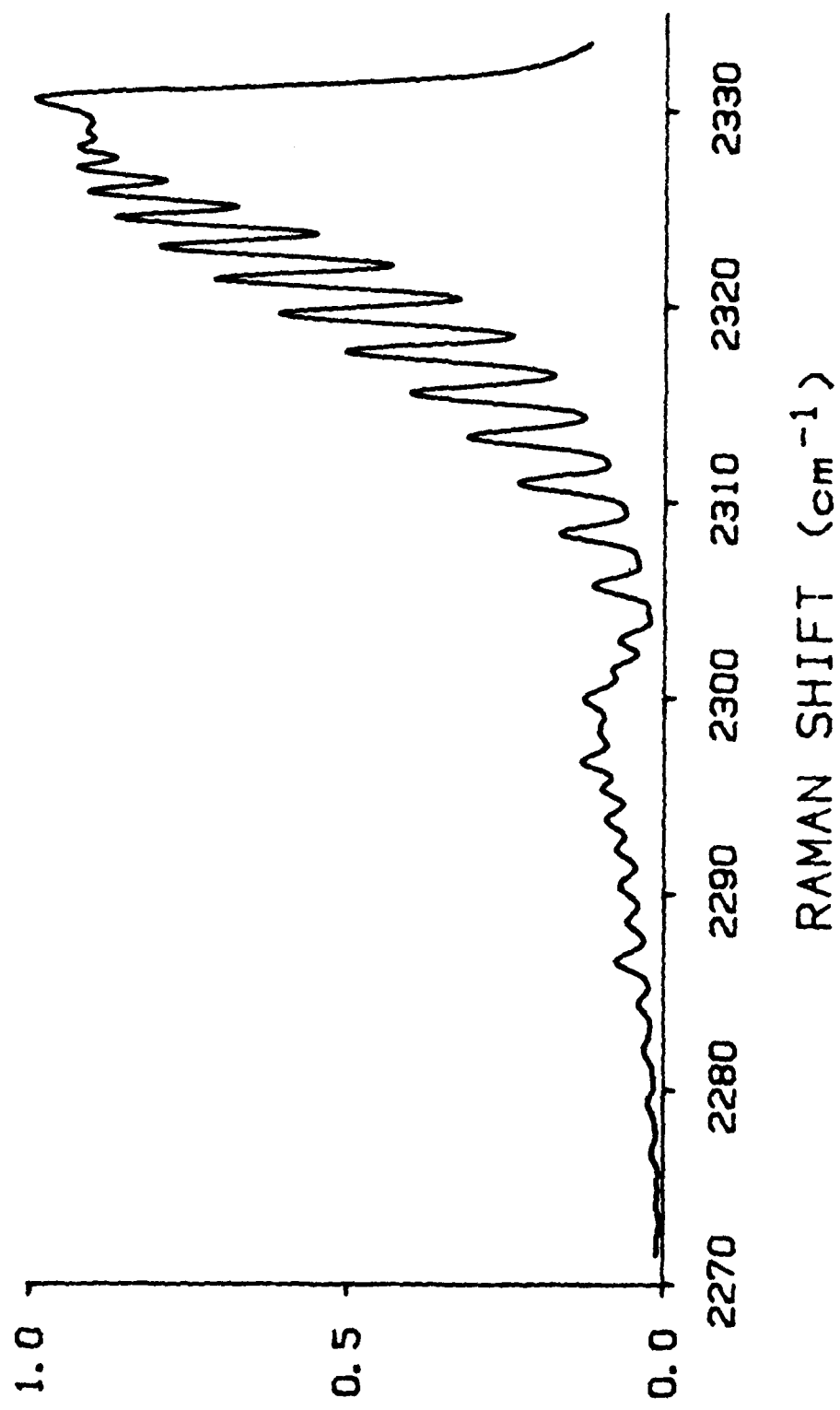


Figure 2 Example of a computed CARS spectrum for N<sub>2</sub> gas at 1700°K.

On the other hand, Moya, et al<sup>39</sup> have made high resolution measurements of fine structure at the top of the ground state band, and our computed high resolution spectra, as well as their own computed spectra, agree very well with this measured fine structure. There is thus good reason to have confidence that our computer code is sound and that the small leading edge peak in Figure 2. is a true part of the spectrum under the conditions assumed by the computer code. One of these conditions is complete absence of any saturation effects, and we believe it is this condition that is not applicable to the UTRC experiments. The intensity in the small peak at the bandhead is due to the first few lines in the Raman band. Since these lines are the lines with the smallest statistical weights, they are the lines that would be most easily saturated. Furthermore, they are positioned spectrally where the CARS intensity is largest and therefore the pumping rate due to stimulated Raman scattering (SRS) is greatest. As a result, these first few lines may be highly saturated even when the band as a whole is almost totally unsaturated.

A first approximation to the effect of partial saturation of a transition is a reduction of its contribution to the susceptibility by a factor of  $1/(1+P/P_{\text{sat}})$  where  $P$  is the SRS pumping rate for the transition and  $P_{\text{sat}}$  is a saturation parameter pumping rate proportional to the statistical weight.  $P$  is proportional to the CARS intensity at the transition frequency, so  $P$  is roughly the same for each of the bandhead lines. We can therefore estimate the effect of saturation on the bandhead by calculation of a spectrum with each line strength multiplied by a factor of  $1/\{1+\alpha/(2J+1)\}$  where  $\alpha$  is a constant. Figure 3. shows such a spectrum computed with  $\alpha = 2.0$  but otherwise with the same parameters as in Figure 2.

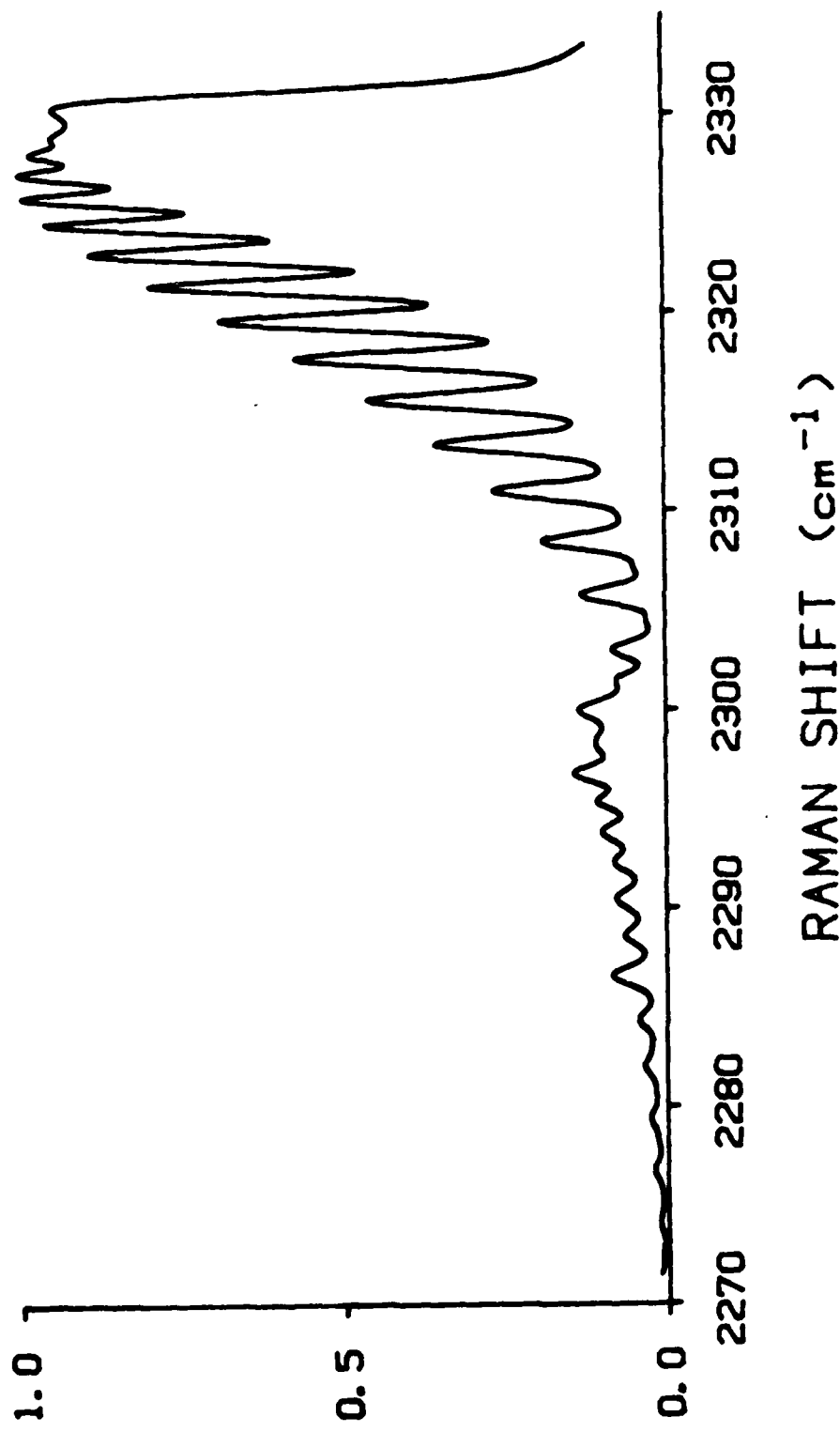


Figure 3 Spectrum computed as in Figure 2 but incorporating bandhead saturation.

Because a smaller pump rate is appropriate for most of the band, this computation substantially overestimates the saturation of the band as a whole. Even so, the calculated saturation based on the reduction in area under the curve (before the two spectra were renormalized for the figures) is only six percent. On the other hand, the value  $\alpha = 2.0$  corresponds to a 67% saturation of the  $J = 0$  line, and even this degree of saturation has not completely eliminated the small bump at the leading edge of the bandhead, although it has been greatly reduced. Using somewhat larger values of  $\alpha$  and somewhat wider ( $1.5 \text{ cm}^{-1}$ ) slit functions, it is possible to generate bandhead shapes that closely resemble the UTRC experimental spectra. This leading edge saturation is not a problem provided other portions of the spectrum are used for comparisons between experimental and computed spectra. In fact, one has at a glance an indication of the degree of saturation, which may prove to be a useful indicator for an experienced operator.

For water vapor calculations, we had available two large sets of data on the frequencies of various Raman active lines. However, the dataset obtained from Prof. Gaufres is of uncertain vintage, and the two datasets do differ slightly where they overlap. We therefore performed some tests of the sensitivity of the computed spectra to the precision of the data. Figure 4. shows the results of one such test. The two curves in Figure 4. are two computed spectra (normalized to the same area under the curves) for the same conditions,  $1700^\circ\text{C}$  and  $50 \times 10^{-3} \text{ cm}^{-1}$  CARS halfwidth parameter. One spectrum was computed using the full melded dataset, whereas the other was computed using a dataset in which the Raman frequencies had been randomly shifted, in this case by an average shift of  $50 \times 10^{-3} \text{ cm}^{-1}$ . For an average shift of this size, Figure 4. shows the test case in which the spectra differ most. The frequencies in

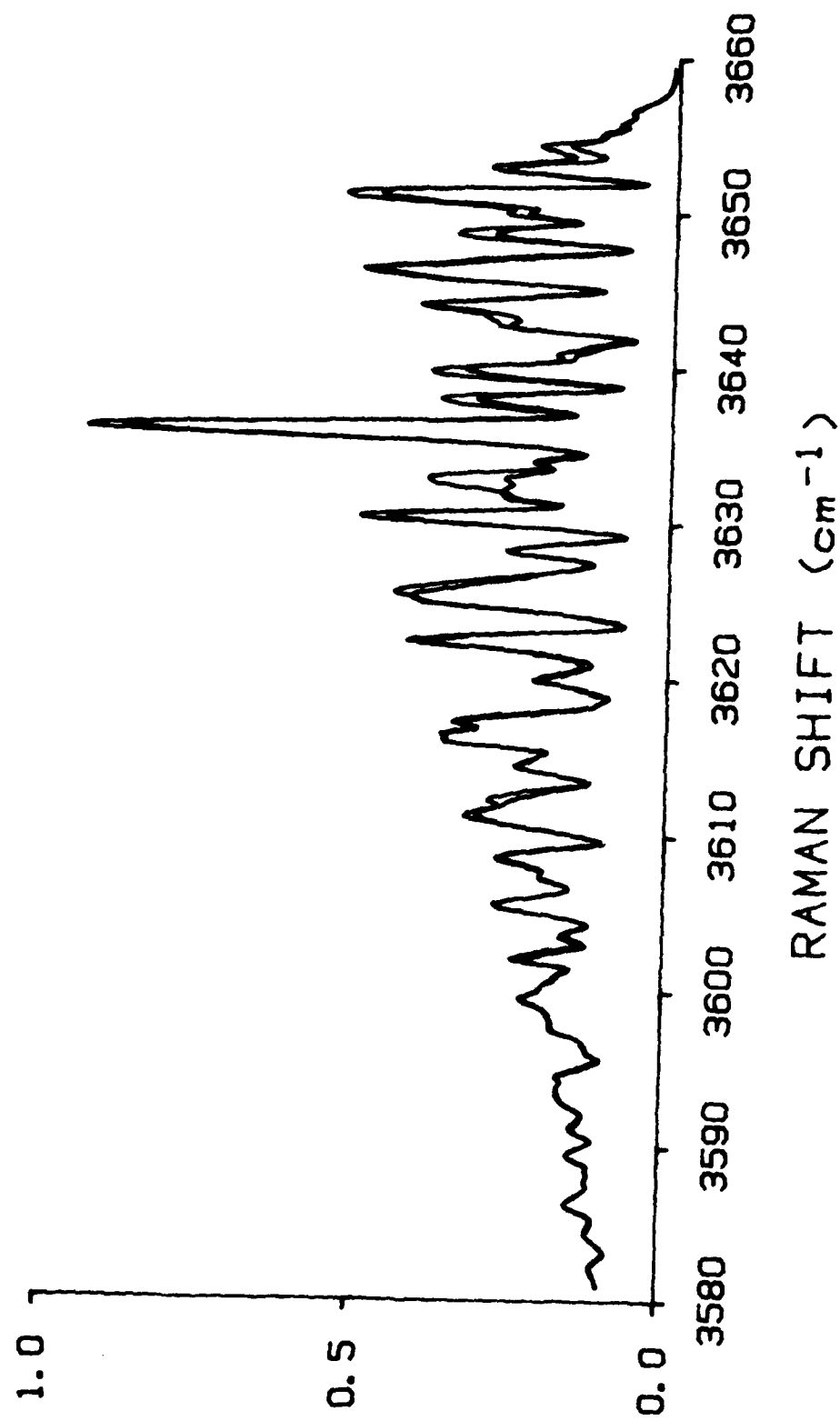


Figure 4 Superimposed water vapor CARS spectra, one with best input and one with randomly shifted input Raman frequencies.

our two datasets generally differ by less than one fifth of this shift for lines where the datasets overlap, although a few weak lines differ by as much as about one  $\text{cm}^{-1}$ . These latter lines are unimportant, and we believe the spectral sensitivity tests show that the differences between the datasets are negligible.

Figure 5. shows our computed water vapor spectrum that comes closest to matching the experimental spectrum of Shirley, Eckbreth, and Hall<sup>36,40</sup> (SEH). The figure displays our computed spectrum with about the same aspect ratio as the published SEH experimental spectrum. In some characteristics, our computed spectrum matches the SEH experimental spectrum better than their own computed spectrum does, most notably in the height of the most prominent feature, the tall peak at about  $3635 \text{ cm}^{-1}$ . However, the SEH computed spectrum shows better agreement than does our Figure 5. in some other details, particularly in the heights of the two major peaks between  $3620$  and  $3625 \text{ cm}^{-1}$ .

The difference in height of the prominent peak at  $3635 \text{ cm}^{-1}$  is probably not inherent in the basic computation of  $|\tilde{x}(\omega)|^2$  but instead is related to the spectral broadening functions. For the SEH experiments with a multimode pump laser, the observed spectrum is the convolution of  $|\tilde{x}(\omega)|^2$ , the pump laser spectral envelope  $S_p(\omega)$ , and the spectrometer slit function  $F(\omega)$ . For the spectrum in Figure 5.,  $F(\omega)$  is triangular with FWHM =  $1.0 \text{ cm}^{-1}$ , and  $S_p(\omega)$  simulates a pump laser spectral envelope  $0.8 \text{ cm}^{-1}$  wide between abrupt edges where the gain curve crosses the loss level. We have found that use of any shape with significant tails, e.g., a gaussian, for either of these broadening functions reduces the prominence of this main spectral feature. Some of the other spectral details are also surprisingly sensitive to the shapes of the broadening functions.

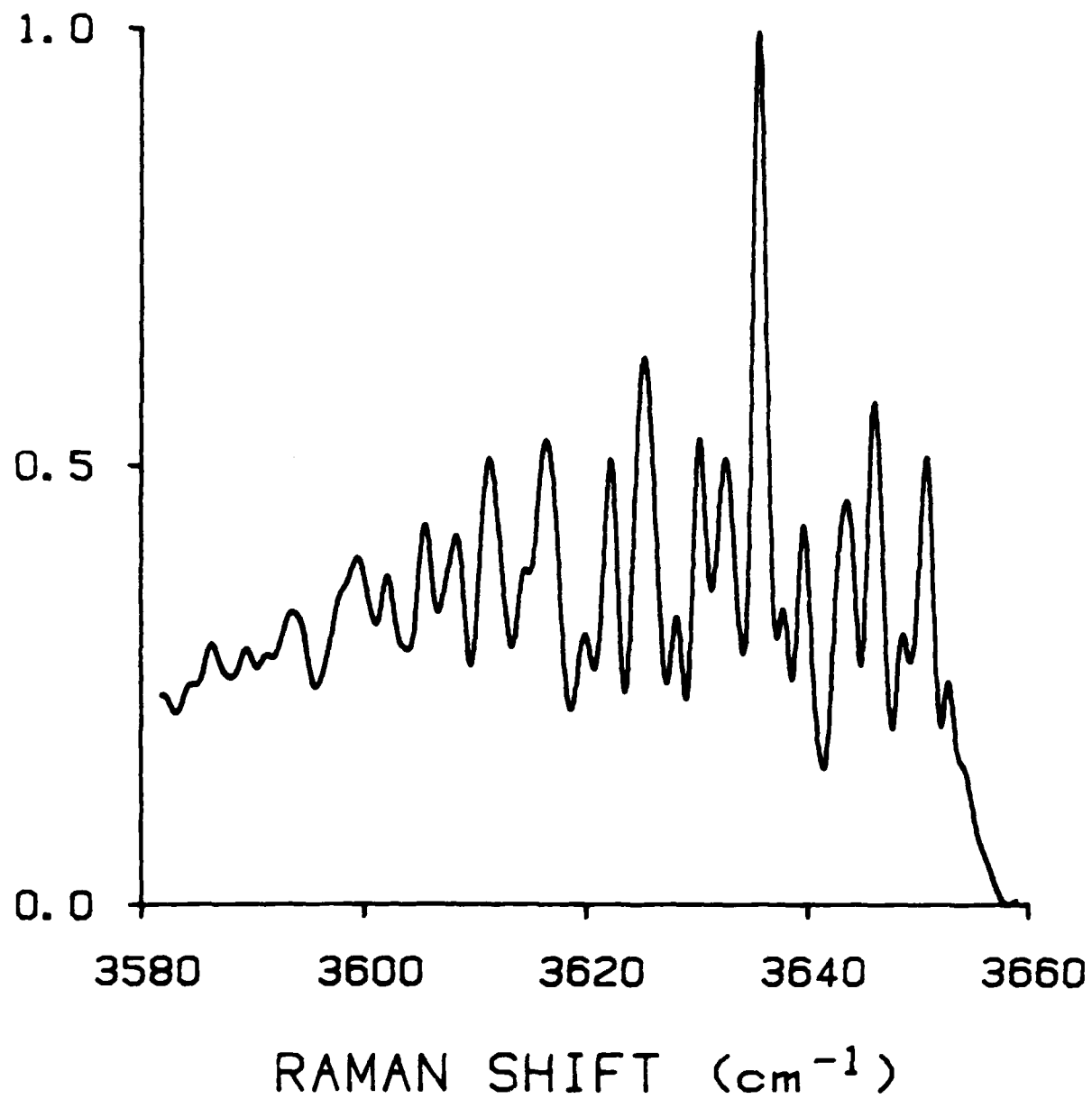


Figure 5 Our best computed match to the experimental water vapor spectrum of Ref. 41.

### III.G Conclusions

The technologically most important conclusion we can draw from this study is that CARS, as a form of spectroscopy, is simpler and should be more generally useful than conventional analyses suggest. However, as a physical process, CARS is considerably more complex and subtle than has been previously recognized. That these seemingly inconsistent statements can be both true is a result of the special statistical properties of optical fields from laser sources.

The very occurrence of CARS is dependent on the "condensed phase" nature of the output of lasers. This optical condensation, similar to other Bose condensation underlying superconductivity and superfluidity, ultimately requires a quantized-field treatment. However, we have chosen to stay as close as possible to the theoretical frameworks common in the CARS literature and to emphasize the physical meaning of the complexity of CARS. We have shown that if we take care to include the statistical structure of the laser fields, we can see that the coherence of a CARS interaction is as much a reflection of the properties of the interacting laser fields as it is a probe of the medium that couples them. For lasers with relatively poor coherence, the coherence of the interaction as represented by the susceptibility linewidth parameter, becomes dominated by the lasers. Having a linewidth parameter known to be constant simplifies the interpretation of CARS spectra and should greatly amplify the ease, range, and reliability of CARS measurements.

Some questions remain, however. For example, we have generally ignored Doppler broadening because, according to the previously accepted literature

expression for CARS Doppler widths, these widths are small enough to be neglected in most cases. A recent publication has presented a different calculation of Doppler broadening. Although there are some dubious aspects of this new calculation, it has at least served to bring out that there may be unexplored issues involved in Doppler broadening of CARS. As other examples, our brief discussions of non-stationarity in the evolving short-pulse laser fields and of the intermode correlations are not likely to be the last words on those topics.

We began the work under this contract with the expectation that the basic theory of CARS was correct as it was presented in the literature and that we would be applying this theory to an analysis of CARS as a diagnostic tool for probing combustion media. What we found, however, is that the literature theory of CARS has serious deficiencies, and our work under this contract has instead consisted of applying our own theory, concurrent with its development under internal corporate funding. A developing theory is never as thoroughly understood as a complete one, and as a result our analysis of the application to combustion diagnostics is in less specific terms than we would have preferred. As a compensating factor, we have been able to discuss points that are important to diagnostics but whose very existence is not suggested by prior theory.

We have also written and delivered the computer programs required under this contract. These are described and listed separately in the previously delivered user's manual for them.

## REFERENCES

1. P. D. Maker and R. W. Terhume, Physical Review, 137, 801 (1965).
2. P. R. Regnier and J.-P. E. Taran, "Gas Concentration Measurements by Coherent Raman Anti-Stokes Scattering," in Laser Raman Gas Diagnostics, M. Lapp and C. M. Penney, eds., (Plenum Press, New York, 1974).
3. For example: W. M. Tolles, J. W. Nibler, J. R. McDonald, or A. B. Harvey, Applied Spectroscopy 31, 253 (1977), and H. C. Andersen and B. S. Hudson, Molecular Spectroscopy, 5, 142 (1978).
4. Robert J. Hall, private communication.
5. Robert J. Hall and Alan C. Eckbreth, Proceedings of the Society of Photo-optical Instrumentation Engineers, 158, 59 (1978).
6. N. Bloembergen, Nonlinear Optics, (W. A. Benjamin, New York 1965).
7. Paul N. Bucher, Nonlinear Optical Phenomena, (Bulletin 2000, Engineering Experiment Station, Ohio State University, Columbus, 1965).
8. R. N. DeWitt, A. B. Harvey and W. M. Tolles, Theoretical Development of Third-Order Susceptibility as Related to Coherent Anti-Stokes Spectroscopy, Naval Research Laboratory memorandum report 3260, (NTIS document AD-AO24-164, 1976).
9. Won B. Roh and Paul W. Screiber, Applied Optics, 9, 1418 (1978).
10. Wilber B. Davenport, Jr. and William L. Root, An Introduction to the Theory of Random Signals and Noise, (McGraw-Hill, New York, 1958).
11. Max Born and Emil Wolf, Principles of Optics, (MacMillan, New York, 1964).
12. Mark J. Beran and George B. Parrent, Jr., Theory of Partial Coherence, (Prentice Hall, Englewood Cliffs, NJ, 1964).
13. Mark J. Beran, Statistical Continuum Theories, (Wiley, New York, 1968).
14. M. A. Yuratich, Molecular Physics, 38, 625 (1979).
15. It is, however, possible to make a statistical distinction between the fields arising from the two types of interaction, which might be relevant if the CARS beam were used as a source in a second experiment.
16. R. L. St. Peters, Optics Letters, 12, 401 (1979).

17. John Orn Bjarnason, Bruce S. Hudson, and Hans C. Andersen, *J. Chemical Physics*, 70, 4130 (1979).
18. R. H. Dicke, *Physical Review*, 89, 472 (1953).
19. M. A. Henesian, L. Kulevskii, R. L. Byer and R. L. Herbst, *Optics Communications*, 18, 224 (1976).
20. S. D. Silverstein, private communication.
21. Albert Messiah, Quantum Mechanics, (Wiley, New York, 1966), vol. I.
22. In past years we have confirmed this by direct measurements on a number of simple molecules.
23. This is implied by the measurements and analysis in C. M. Penney, R. L. St. Peters and M. Lapp, *J. of the Optical Society of America*, 64, 712 (1974) along with the theory of Ref. 25.
24. Gerhard Herzberg, Molecular Spectra and Molecular Structure II: Infrared and Raman Spectra, (Van Nostrand, Princeton, 1945).
25. G. Placzek, in Handbuch der Radiologie, Vol. 6, G. Marx, ed. (Akademische Verlagsgesellschaft, Leipzig, 1934). (English Translation by A. Werbin, U.C.R.L. Translation No. 526 (L), Lawrence Radiation Laboratory, 1959).
26. J. L. Bribes, R. Gaufres, M. Monan, M. Lapp and C. M. Penney, Proceedings of the Fifth International Conference on Raman Spectroscopy, E. E. Schmid, et. al. eds. (Hans Ferdinand Schulz Verlag, Freiburg, 1976).
27. J. M. Flaud, C. Camy-Peret, and J. P. Maillard, *Molecular Physics*, 32, 499 (1976).
28. C. Camy-Peret and J. M. Flaud, *Molecular Physics*, 32, 523 (1976).
29. C. Camy-Peret and J. M. Flaud, *J. of Molecular Spectroscopy*, 67, 117 (1977).
30. J. Fiutak and J. Van Kronendonk, *Canadian J. of Physics*, 40, 1085 (1962); J. Fiutak and J. Van Kronendonk, *Canadian J. of Physics*, 41, 21 (1963); J. Van Kronendonk, *Canadian J. of Physics*, 41, 433 (1963); C. G. Gray and J. Van Kronendonk, *Canadian J. of Physics*, 44 2411 (1966).
31. R. P. Srivastava and H. R. Zaida, *Canadian J. of Physics*, 55, 533, 542, and 549 (1977).
32. The elastic collisions that change  $M$ , resulting in a small phase interrupt broadening of non-trace Raman scattering must be distinguished from the elastic collisions of Section II.E, which change only the translation state, leaving even  $M$  unchanged and resulting in no collisional broadening.

33. K. S. Jammu, G. E. St. John, and H. L. Welsh, Canadian J. of Physics, 44, 797 (1966).
34. William H. Fletcher, letters of September 29 and October 10, 1978 to M. Lapp forwarded to the author.
35. A. Owyong and L. A. Rahn, 1979 Conference on Laser Engineering and Applications, Washington, DC, May/June 1979.
36. John A. Shirley, Alan C. Eckbreth, and Robert J. Hall, Investigation of the Feasibility of CARS Measurements in Scramjet Combustion, Technical Report on Contract NASI-15491 for NASA Langley Research Center, (United Technologies Research Center report R79-954390-8, East Hartford, CT, 1979).
37. Gerhard Herzberg, Molecular Spectra and Molecular Structure I: Spectra of Diatomic Molecules, (Van Nostrand, New York, 1950).
38. For example, see Refs. 5 and 34.
39. F. Moya, S. Druet, M. Pealat, and J.-P. E. Taran, in Laser Spectroscopy, S. Haroche, et. al., eds.,, (Springer-Verlag, New York, 1975), or see W. M. Tolles et. al., Ref. 3.
40. Robert J. Hall, John A. Shirley, and Alan C. Eckbreth, Optics Letters, 4, 87 (1979).

**DAI**  
**FILM**